



# Tectonics

## RESEARCH ARTICLE

10.1029/2018TC005116

### Key Points:

- The first geological map of 1.5-Mkm<sup>2</sup> submerged South Zealandia reveals an E-W striking batholith with similar age pattern to Marie Byrd Land
- The 1,600-km-long Campbell Magnetic Anomaly System is interpreted as due to failed rift mafic magmatism that preceded 80 Ma Zealandia breakup
- Variation of extension direction over 20 Ma allowed this large area to thin considerably before breakup and formation of new oceanic crust

### Supporting Information:

- Supporting Information S1

### Correspondence to:

Andy J. Tulloch,  
a.tulloch@gns.cri.nz

### Citation:

Tulloch, A. J., Mortimer, N., Ireland, T. R., Waight, T. E., Maas, R., Palin, J. M., et al. (2019). Reconnaissance basement geology and tectonics of South Zealandia. *Tectonics*, 38, 516–551. <https://doi.org/10.1029/2018TC005116>

Received 24 APR 2018

Accepted 29 DEC 2018

Accepted article online 4 JAN 2019

Published online 8 FEB 2019

## Reconnaissance Basement Geology and Tectonics of South Zealandia

Andy J. Tulloch<sup>1</sup> ID, Nick Mortimer<sup>1</sup> ID, Trevor R. Ireland<sup>2</sup> ID, Tod E. Waight<sup>3</sup> ID, Roland Maas<sup>4</sup> ID, J. M. Palin<sup>5</sup> ID, Tusar Sahoo<sup>6</sup> ID, Hannu Seebeck<sup>6</sup>, Matt W. Sagar<sup>6</sup> ID, Andrea Barrier<sup>7</sup> ID, and Rose E. Turnbull<sup>1</sup> ID

<sup>1</sup>GNS Science, Dunedin, New Zealand, <sup>2</sup>Research School of Earth Science, Australian National University, Canberra, ACT, Australia, <sup>3</sup>Department of Geosciences and Natural Resources Management (Geology Section), University of Copenhagen, Copenhagen, Denmark, <sup>4</sup>School of Earth Sciences, University of Melbourne, Parkville, Victoria, Australia,

<sup>5</sup>Department of Geology, University of Otago, Dunedin, New Zealand, <sup>6</sup>GNS Science, Lower Hutt, New Zealand,

<sup>7</sup>Department of Geosciences, University of Canterbury, Christchurch, New Zealand

**Abstract** We report new U-Pb zircon ages, geochemical and isotopic data for Mesozoic igneous rocks, and new seismic interpretations of mostly submerged South Zealandia (1.5 Mkm<sup>2</sup>). We use these data, along with existing geological and geophysical data sets, to refine the extent and nature of geological units. Our new 1:25 M geological map of South Zealandia provides a regional framework to investigate the rifting and breakup that formed Zealandia, Earth's most submerged continent. Samples of prerift (pre-100 Ma) plutonic rocks can be matched with on-land New Zealand igneous suites and indicate an east-west strike for the subduction-related 260 to 105-Ma Median Batholith across the Campbell Plateau. The plutonic chronology of formerly contiguous plutonic rocks in West Antarctica reveals similar pulses and lulls to the Median Batholith. Contrary to previous interpretations, the Median Batholith does not coincide with the 1,600-km-long Campbell Magnetic Anomaly System. Instead we interpret the continental magnetic anomalies to represent a mainly mafic igneous unit, whose shape and extent is controlled by synrift structures related to Gondwana breakup. Correlatives of some of these unsampled igneous rocks may be exposed as circa 85 Ma alkalic volcanic rocks on the Chatham Islands. Extension directions varied by up to 65° from 100 to 80 Ma, and we suggest this allowed this large area to thin considerably before final rupture to form new oceanic crust. Synrift (90–80 Ma) structures cut the oroclinal bend in southern South Island and support a pre-early Late Cretaceous age of orocline formation.

### 1. Introduction

Zealandia is a 4.9-Mkm<sup>2</sup>, 94% submerged continent located in the SW Pacific Ocean and was formerly part of Gondwana (Mortimer, Campbell, et al., 2017). There are several first-order questions posed by Zealandia as the thinnest (crust) end-member of continents (12–24 km; Grobys et al., 2008; Mortimer, Campbell, et al., 2017). How is it possible to extend continental lithosphere over such wide areas before rupture? Can Zealandia's fringes be compared with typical volcanic-rifted or magma-poor continental margins? Why is West Antarctica (much of which is also highly thinned and a former part of Gondwana; Chaput et al., 2014) not a part of Zealandia? Answers to these questions require a knowledge of the crystalline basement geology of the southern part of the Zealandia continent (Figure 1).

South Zealandia is an ~1.5 Mkm<sup>2</sup> region of continental crust on the Pacific Plate (the only other continental crust on the Pacific Plate is in coastal California and Baja California; Mortimer, Campbell, et al., 2017). South Zealandia includes the South Island of New Zealand, the Chatham Rise, and Campbell Plateau (Figure 1). Pre-Cenozoic geological samples are available from only 21 scattered locations in six island groups (Chathams, Snares, Auckland, Campbell, Bounty, and Antipodes), nine petroleum exploration wells (Clipper-1, Takapu-1, Solander-1, Rakiura-1, Pukaki-1, Pakaha-1, Parara-1, Hoiho-1C, and Kawau-1), and six dredge sites (Takahe and Stuttgart seamounts, Mernoo and Matheson banks, Bounty Platform, and southern Campbell Plateau tip; Figure 1). Submarine basement exposure is limited because a widespread Cenozoic sediment drape over the generally relatively low-relief Campbell Plateau hinders dredging (Summerhayes, 1969). Rocks from most of the above localities have been described previously (Adams, 1983, 2008; Adams & Robinson, 1977; Adams et al., 2008; Beggs, 1978; Beggs et al., 1990; Cook et al., 1999; Cullen, 1965, 1975; Denison & Coombs, 1977; Field & Browne,

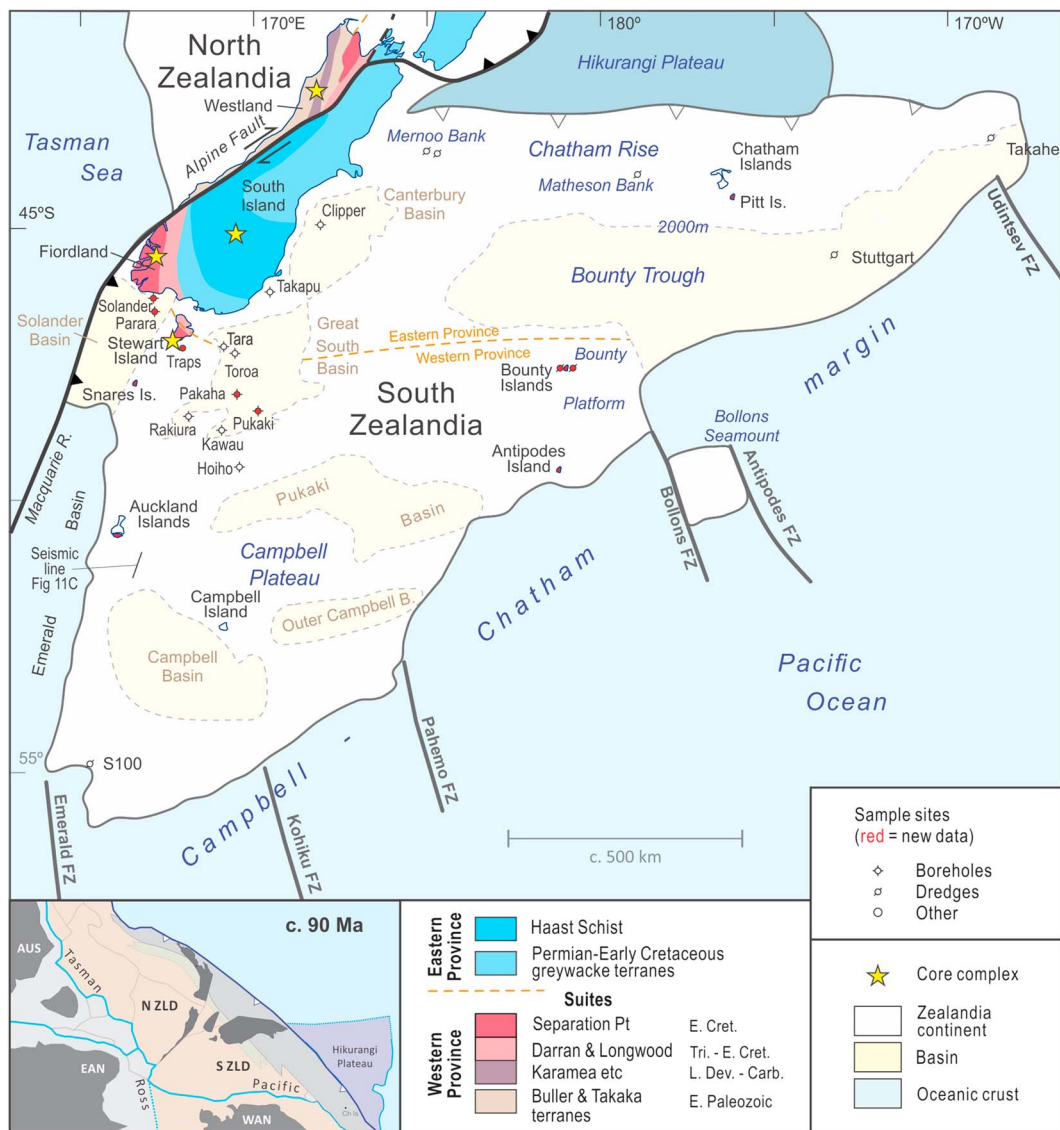


**Figure 1.** Location map of South Zealandia, highlighting samples used in this study. Inset map shows location of South Zealandia at 90 Ma, within a partly stretched continental ribbon on the SE Gondwana margin (ZLD = proto-Zealandia; WAN = West Antarctica; EAN = East Antarctica; AUS = Australia). Blue lines represent future breakup. Hikurangi oceanic plateau is jammed in a Triassic-Early Cretaceous subduction margin. The Eastern Province comprises terranes representing an accretionary wedge and forearc basin associated with Triassic-Early Cretaceous subduction. Western Province comprises Early Paleozoic metasedimentary terranes, intruded by mid-Paleozoic and Triassic-Early Cretaceous continental margin arc batholiths. Boreholes are detailed in Cook et al. (1999).

1989; Fleming et al., 1953; Mortimer et al., 2006, 2016; Scott et al., 2015; Watters & Fleming, 1975, and references therein).

The purpose of this paper is to report new geochemical and U-Pb zircon age data from Mesozoic igneous rock samples of South Zealandia distant from the South Island of New Zealand. The samples were obtained from rock exposures on Bounty, Snares, Auckland, and Chatham Islands; two granite xenoliths in Pleistocene lavas on Antipodes Island; and Pukaki-1, Pakaha-1, and Parara-1 exploration drill holes in the Great South basin. In addition, we report complementary data from the Colbeck Trough in formerly contiguous West Antarctica.

We use the new analytical data in conjunction with other geological and geophysical data to present a new map of the geological basement of South Zealandia. In turn, this map tests and clarifies several

regional geological and tectonic issues, including along-strike orogen-scale similarities and differences with formerly adjacent West Antarctica. A more accurate representation of pre-Gondwana breakup basement geology helps identify and constrain rift-related units and structures. Regarding the latter, we present a new, qualitative interpretation of the Campbell Magnetic Anomaly System (CMAS) and propose that it is the magnetic response of Late Cretaceous, Gondwana-Zealandia synrift-related igneous rocks rather than Paleozoic-Early Cretaceous basement. Late Cretaceous kinematic data from across Zealandia reveal consistently changing patterns of extension, and we present a tectonic model that explains these patterns and the reasons for breakup occurring where it did. This paper is a follow-up to the recently published thermochronology work on South Zealandia (Mortimer et al., 2016). It also succeeds and updates earlier publications on the geology of the Campbell Plateau and Chatham Rise (e.g., Beggs et al., 1990; Cook et al., 1999).

In this paper, we use South and North Zealandia (Mortimer, 2018; Figure 1) rather than the informal southern and northern Zealandia. This style follows East and West Antarctica and emphasizes that Zealandia and Antarctica are both substantially internally deformed.

### 1.1. Geological Background

The geological basement of the South Island and Stewart Island comprises nine Cambrian to Early Cretaceous metasedimentary terranes and three major batholiths, grouped into Eastern and Western provinces (Mortimer, 2004; Mortimer et al., 1999, 2014). These potentially strike across the Campbell Plateau and/or Chatham Rise. The Western Province likely forms much of the southern two thirds of the Campbell Plateau and is composed of two Early Paleozoic terranes, Buller and Takaka. Buller Terrane lies to the west and south of Takaka Terrane, toward the Gondwana interior, and consists of low-grade siliciclastic sandstones and mudstones. Takaka Terrane consists of siliciclastic, carbonate, and volcanic rocks of Cambrian-Early Devonian age. The Eastern Province terranes represent growth of Gondwana in accretionary complexes during Permian-Cretaceous subduction (Mortimer, 2004, and references therein). The batholiths are the magmatic arc record associated with episodes of subduction-related (I-type granitoids) and episodes of nonsubduction (A-type granitoids). Below we describe the main geological units and their boundaries that are relevant to this paper.

The northern edge of South Zealandia is at the foot of the northern side of the Chatham Rise where it abuts the Hikurangi Plateau Large Igneous Province (Davy et al., 2008; Herzer & Wood, 1988; Mortimer et al., 2006). This continent-ocean boundary (COB) is the surface expression of the fossil Cretaceous subduction zone and is possibly the only unmodified Cretaceous subduction margin in the entire circum-Pacific. The Chatham Rise is an east-west 1,500-km-long feature that terminates against the South Island between Christchurch and Kaikoura. In this part of the South Island, rocks of the Torlesse Composite Terrane (Eastern Province) are exposed. Torlesse rocks comprise structurally imbricated Carboniferous to Early Cretaceous feldspatholithic sedimentary successions (e.g., MacKinnon, 1983) with minor interfaulted bands of a basalt-chert-argillite association.

Torlesse greywacke and schist are present on the Chatham Islands (Adams et al., 2008; Adams & Robinson, 1977), and Torlesse rocks have also been sampled on the Chatham Rise (Cullen, 1965). Permian-Triassic Maitai and Caples terranes formed in near-arc, lower trench slope settings prior to juxtaposition with Torlesse Terrane. Collectively the Torlesse Composite and Caples terranes represent an exhumed Mesozoic accretionary wedge. The Caples-Torlesse boundary has been metamorphosed (Haast Schist) within the accretionary wedge. In South Island, Murihiku Terrane (Eastern Province) is a well-preserved, fossiliferous, little-deformed, Late Permian to Middle Jurassic sedimentary basin. Strata are folded into broad upright synclines and anticlines. Murihiku Terrane is commonly interpreted to be the forearc basin to the Mesozoic accretionary wedge (Mortimer, 2004).

A Mesozoic magmatic arc, the Median Batholith (Mortimer et al., 1999; Mortimer et al., 2002; Muir et al., 1998; Tulloch & Kimbrough, 2003), is well exposed in Nelson, Fiordland, and Stewart Island. It lies on the eastern edge of the Western Province (Scott, 2013) and comprises two parallel plutonic belts, a north-eastern (Pacificward) Permian to Early Cretaceous (ca. 260–135 Ma) belt of mainly gabbros, diorites, and granodiorites and a southwestward (Gondwanaward) Early Cretaceous (ca. 130–105 Ma) belt of mainly granite-diorite plutons of the Separation Point Suite, which have a strong adakitic character (Muir

et al., 1995; Schwartz et al., 2017; Tulloch & Kimbrough, 2003; Tulloch & Rabone, 1993). Here we use the term “adakitic” to describe granitic-dioritic rocks with elevated Sr/Y compositions; we are not referring to classic adakites generated by slab melting (see nomenclature discussion in Tulloch & Kimbrough, 2003). The deep Cretaceous crust (up to 60 km, De Paoli et al., 2009) of the latter is exposed in Fiordland, and the adakitic inboard belt has been inferred to have supported significant paleotopography in the Early Cretaceous, termed Cordillera Zealandia by Tulloch et al. (2006). To the south and west of the contiguous Median Batholith (inboard relative to the Cretaceous margin), Separation Point Suite plutons also intrude Early Paleozoic, typically quartzose metasedimentary Buller and Takaka Terranes (e.g., Cooper, 1989; Cooper & Tulloch, 1992; Münker & Cooper 1999). In the western, Buller Terrane, Separation Point Suite magmas incorporated continental crust to produce the subweakly adakitic Rahu Suite (Tulloch, 1988; Tulloch & Kimbrough, 2003; Waught et al., 1998). Relatively homogenous Sr-Nd isotopes in this suite in the Hohonu Ranges constrain such incorporation to the lower crustal source region of the magmas (van der Meer et al., 2018). The Rahu Suite has similar age range, ca 130–101 Ma (Revolver, Brothers, ca. 131–115 Ma, etc. in Allibone et al., 2007; Hohonu Ranges, 114–109 Ma in Waught et al., 1997; Canavans quartz monzogranite, 101 Ma in Tulloch, Ramezani, Mortimer, et al., 2009; van der Meer et al., 2018) to the Separation Point Suite (ca. 126–105 Ma in Tulloch & Kimbrough, 2003). A separate, Devonian-Carboniferous Karamea Batholith in Buller Terrane is dominated by Karamea Suite S-type granite that was generated during a major latest Devonian flare-up event that is also recognized in SE Australia and West Antarctic sectors of the SE Gondwana margin (Tulloch, Ramezani, Kimbrough, et al., 2009; Tulloch et al., 2017; R. Turnbull et al., 2016).

Continental extension that led to breakup of Zealandia with Australia and Antarctica has previously been reported in Nelson (North Zealandia; Tulloch & Kimbrough, 1989; Klepeis et al., 2007; Schulte et al., 2014), Fiordland (Gibson et al., 1988), and Stewart Island (Kula et al., 2007, 2009). Regional intraplate extension affected *both* North and South Zealandia from circa 100 to circa 80 Ma. However, extension in North Zealandia was apparently dominated by 100–93 Ma (Spell et al., 2000; Tulloch, Ramezani, Mortimer, et al., 2009) stretching approximately normal to Tasman Sea whereas extension in South Zealandia was dominated by 92–80 Ma (Kula et al., 2007) stretching approximately normal to the Pacific Ocean margin. These events are discussed in detail below (section 4.4), including discussion of previous suggestions that extension initiated as old as 110 Ma.

Possible Takaka Terrane (or older) equivalents have been reported from greywacke and schist on Campbell Island (Adams, 2008). A Precambrian K/Ar age for a granite dredged from the southernmost tip of Campbell Plateau (site S100) was reported by Challis et al. (1982) and its age confirmed in a U-Pb study by Adams et al. (2015). However, the low-temperature thermochronological study by Mortimer et al. (2016) interpreted the sample as an Antarctic-derived dropstone and, thus, not part of an *in situ* Campbell Plateau pluton. No other Precambrian rocks are recognized in Zealandia.

Seven postaccretionary, intracontinental sedimentary basins are present in South Zealandia. These are Bounty Trough, Canterbury, Great South, Solander, Pukaki, Campbell, and Outer Campbell basins (Figure 1). Great South basin has up to 8.6 km thickness of sedimentary rocks, of which up to 4 km are Late Cretaceous in age (Cook et al., 1999; Sahoo et al., 2014). The basin is controlled on its NW side by the 89–80 Ma Sisters detachment fault (Kula et al., 2007, 2009) of the Pegasus Metamorphic Core Complex (Ring et al., 2015). Canterbury Basin deepens east into the bathymetric Bounty Trough. All basins, particularly the Bounty Trough and Great South basin, represent places where Gondwana continental crust was significantly thinned (to 9 and 13 km, respectively; Grobys et al., 2007, 2008) and rifted prior to breakup of (and formation of oceanic crust between) the Campbell Plateau and West Antarctica (e.g., Davy, 1993; Davy, 2014; Grobys et al., 2008; Mortimer et al., 2019; Wood & Anderson, 1989). Despite the relative youth of exposed Zealandia crust several authors report that the subcontinental lithosphere includes domains that preserve ancient (ca. 1.6–1.9 Ga) melt extraction events (Liu et al., 2015; McCoy-West et al., 2013; Scott, Hodgkinson, et al., 2014; Scott, Waught, et al., 2014). McCoy-West et al. (2016) and van der Meer et al. (2017) both suggest Zealandia-wide enrichment of the lithospheric mantle from circa 100 Ma forming a potential lithospheric source for intraplate lavas.

Virtually all New Zealand terranes and batholiths have been deformed by a large Z-shaped orocline that dominates large scale on-shore geology, recently reviewed by Mortimer (2014).

## 1.2. Continental Magnetic and Gravity Anomalies

In the general absence of rock samples, magnetic anomalies have been used to interpolate and extrapolate Campbell Plateau basement geology (Figure 2). Davey and Christoffel (1978) and Grindley and Davey (1982) defined a set of long-wavelength NE-SW trending anomalies in the eastern Campbell Plateau as the CMAS. They, with caveats (Grindley & Davey, 1982) and Sutherland (1999), correlated the CMAS with the distinctive Stokes Magnetic Anomaly System (SMAS) of onshore and nearshore New Zealand (Hunt, 1978). A consequence of such a correlation is the inferred presence of an otherwise unsubstantiated dextral fault, the Campbell Fault (Figure 2), with ~350-km offset between the SMAS and CMAS, that continues to feature in interpretations (e.g., Davy, 2014). However, there have been alternative interpretations. Beggs et al. (1990) questioned the existence of the Campbell Fault on the basis that relatively quartzose Western Province meta-sedimentary rocks lie northeast of the CMAS but southwest of the SMAS. Based on multichannel seismic velocity models, Grobys et al. (2008) suggested that the SMAS and CMAS have different origins. Several sets of gravity lineations are present on the Campbell Plateau (Figure 3), one of which is coincident with the CMAS.

## 2. Sample Descriptions and Analytical Results

Samples with prefixes P and R and prefix OU are archived in the GNS Science and University of Otago Department of Geology collections, respectively. All sample data are lodged in the Petlab database <https://pet.gns.cri.nz/pet/>; location details are also reported in supporting information Table S1. Drill hole samples are cuttings (except Solander-1), with the usual issues and caveats regarding downhole contamination from cavings, etc. Geochemistry and geochronology samples were handpicked for apparent contamination. Nevertheless, on the scale of this study, we consider that the material is representative of basement rocks either in situ or locally present. In the following we describe the geology, geochronology, and geochemistry of the samples based on their geographic location and present each in a series via an anticlockwise loop from Stewart Island to Great South basin, Auckland and Snares Islands to Antipodes Island and Bounty Island, and finishing at Pitt Island in the northeast of South Zealandia. All plutonic rocks are peraluminous, and all but two granodiorites have  $\text{SiO}_2 > 71\%$ . Suites are primarily defined here on the basis of geochemistry; age information is a secondary consideration (Tulloch, 1988). Photomacrographs of thin sections of most samples are provided in the supporting information Figure S1. Whole-rock X-ray fluorescence (XRF) major and trace element geochemical data along with magnetic susceptibility measurements are reported in Table 1.

Calibration standards for U-Pb geochronology are as follows. Laser ablation inductively coupled plasma mass spectrometry (LA-ICPMS) at Otago University used Temora-2 (417 Ma; Black et al., 2003); sensitive high-resolution ion microprobe (SHRIMP) analyses used AS3 (1099 Ma) and SL13 (572 Ma), both of which are discussed in Black et al. (2003). Standards used for individual samples are listed with analyses in Table S2. Full details of all analytical methods and all analytical data are reported in the supporting information (Bouvier et al., 2008; Getty & Gromet 1992; Horstwood et al., 2016; Ireland & Williams 2003; Jaffey et al., 1971; Jochum et al., 2011; Krogh 1982; Maas et al., 2015; Muir et al., 1996; Paton et al., 2010, 2011; Scott, Hodgkinson, et al., 2014; Scott, Waight, et al., 2014; Steiger & Jäger 1977).

### 2.1. Stewart Island and the Traps

Stewart Island is predominantly composed of Carboniferous-Early Cretaceous granitic-dioritic rocks (Allibone & Tulloch, 2004, 2008), with the youngest granite dated at 105 Ma (Tulloch & Kimbrough, 2003). A major fault system, the Sisters Shear Zone (Kula et al., 2007, 2009; Ring et al., 2015) exhumed mid-crust along an ~70° trending detachment fault that dips ~20° SSE. The fault is parallel or subparallel to much of the eastern margin of the Campbell Plateau and cessation of rapid exhumation of the footwall, determined by  $^{40}\text{Ar}/^{39}\text{Ar}$  thermochronometry on K-feldspar at 78 and 83 Ma (two analyses from Kula et al., 2009), overlaps Campbell Plateau-West Antarctica breakup and formation of new ocean crust at or just before chron 330 (79 Ma; Cande & Stock, 2004), that is, circa 80 Ma.

The Traps, exposed in reefs ~35 km offshore SE Stewart Island (Figure S2), are composed of massive, undeformed medium-grained (~3 mm) biotite quartz monzonite situated in the hanging wall of the Sisters Shear Zone (Kula et al., 2007). Biotite is brown, K-feldspar is perthitic, small titanite lozenges are common, and zircon forms squat prisms.

LA-ICPMS analysis of zircon from The Traps yielded 39 satisfactory analyses (Table S1 and Figure 4). The weighted mean of all analyses is  $122.7 \pm 1.0$  Ma with an MSWD (mean square weighted deviation) of 5.2.

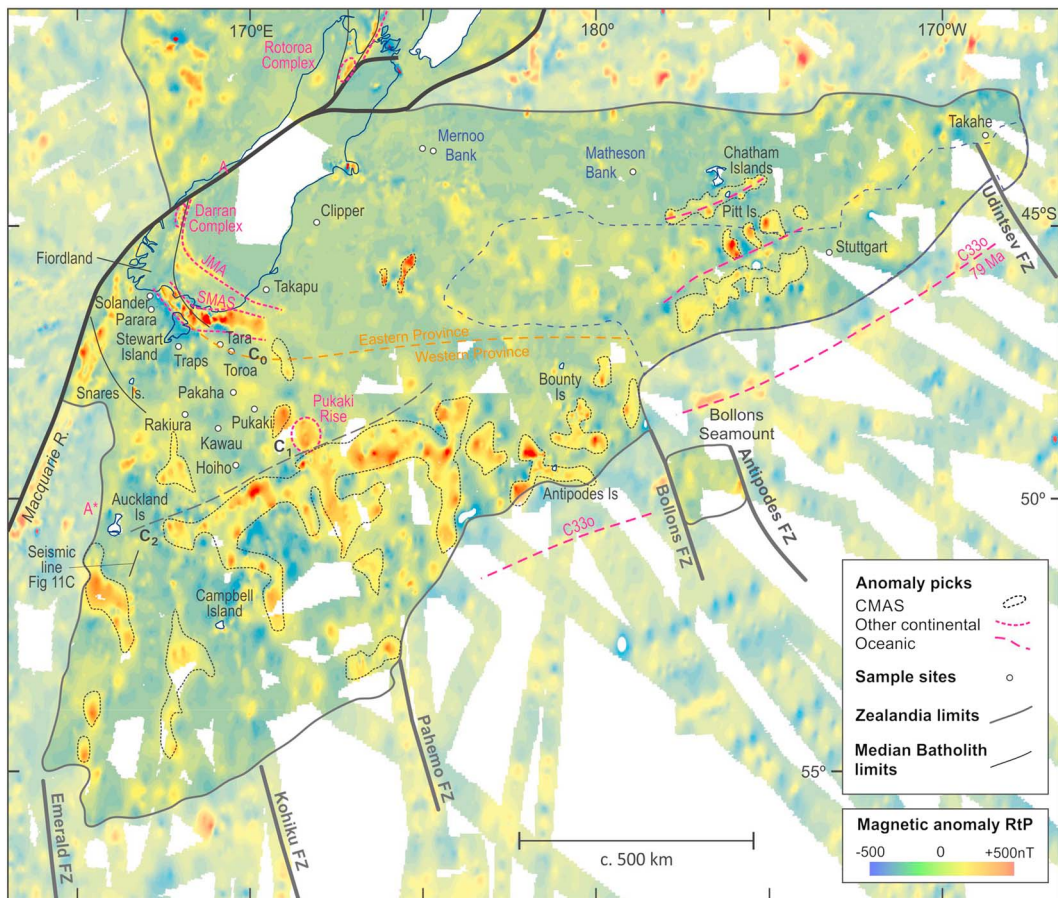


**Figure 2.** Magnetic map of South Zealandia. Based on Sutherland (1999) and data held by GNS Science. Most of Median Batholith has a much lower magnetic expression than the CMAS (fine black picks), extended herein to include similar anomalies immediately south of Chatham Island. CMAS = Campbell Magnetic Anomaly System; SMAS = Stokes Magnetic Anomaly System; JMA = Junction Magnetic Anomaly. Previous authors (e.g., Sutherland, 1999) have projected Paleozoic-Mesozoic continental margin arc rocks from C<sub>0</sub> to C<sub>1</sub> where it is offset along a putative dextral Campbell Fault (dashed line) to C<sub>2</sub>. HIMU-like basalts dredged from Pukaki Rise are Pliocene in age (Timm et al., 2010) and suggest that at least some of the magnetic rocks within the CMAS are not (directly) related to Late Cretaceous rifting.

Gaussian deconvolution (Ludwig, 2011) yields  $122.3 \pm 0.7$  Ma for the major peak, with subsidiary peaks at 128 and 119 Ma. All three ages fall within Early Cretaceous Separation Point and Rahu Suite events; we interpret the crystallization age to be 122 Ma and the 128 and 119 Ma ages to represent inheritance and Pb loss associated with ongoing magmatism within the batholith, respectively. The geochemical analysis (Tables 1 and 2) plots in the alkali-calcic field on the modified alkali-lime index classification of Frost et al. (2001). Low Sr/Y (Figure 5c), elevated Y + Nb (Figure 6) and Ga/Al (2.8 vs. 2.6 for the Whalen et al. (1987) I, S-type/A-type boundary), and a relatively flat, heavy REE (rare earth element)-enriched pattern (Figure 6g) is interpreted as Rahu Suite, albeit possibly transitional to an A-type character (e.g., Dahlquist et al., 2010). Low Sr/Y compared to Rahu Suite is likely due to low Sr rather than high Y. this might suggest assimilation of Paleozoic metasedimentary rock, but this may be contradicted by Sr-Nd isotopes. Relatively primitive  $\epsilon_{\text{Nd}_i}$  of -2.0 is distinctly less enriched than Rahu Suite samples from the Hohonu Range ( $\epsilon_{\text{Nd}_i}$  of -4 to -6; Waight et al., 1998; Figure 7).

## 2.2. Great South and Solander Basin Basement Samples

Four exploration wells reached basement in the Great South basin (Cook et al., 1999), namely, Hoiho-1, Kauau-1, Pakaha-1, and Pukaki-1 (Figure 1). Basement core at total depth in Pukaki-1 was apparently not archived in the government core store by the well operator, so cuttings were used instead. Rakiura-1 and Toroa-1 terminated in Zealandia Megasequence and so, probably, did Tara-1. Previous descriptions

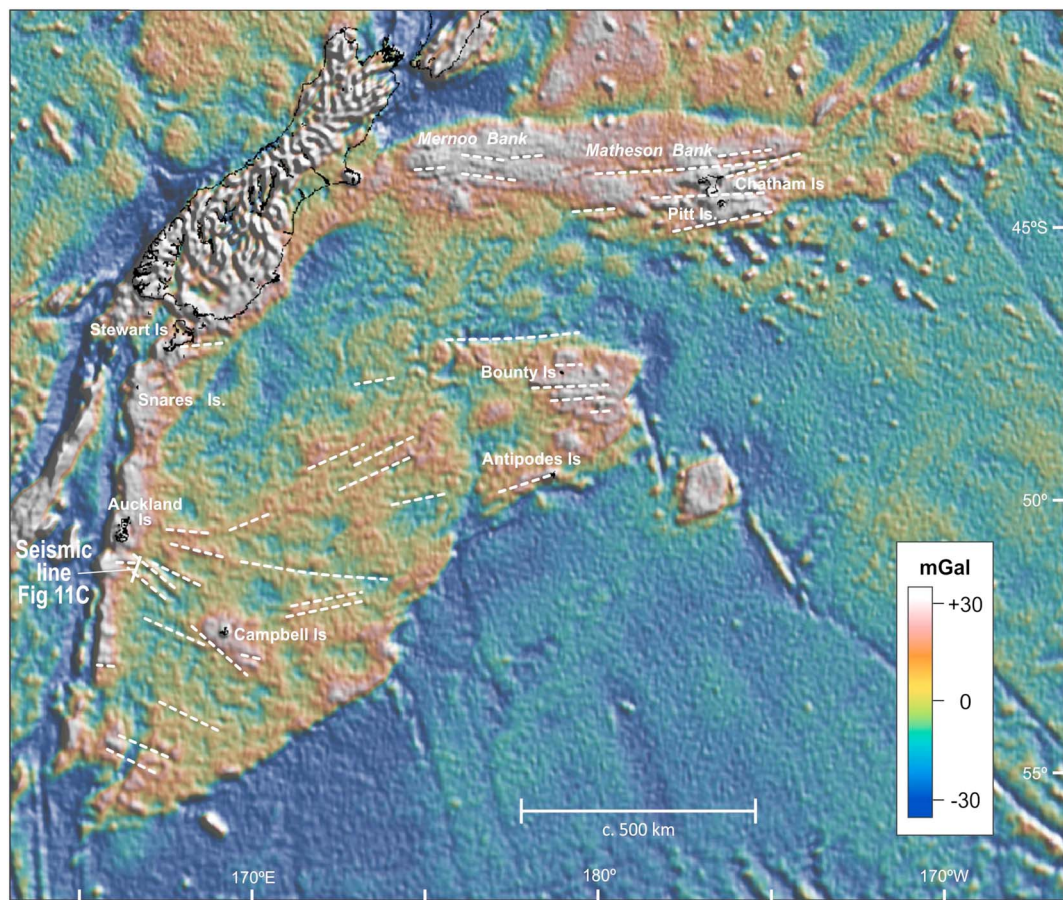


**Figure 3.** Free-air gravity map of South Zealandia (Sandwell & Smith, 1997) with the most significant linear anomalies, and the location of seismic line 11C, denoted.

and lithostratigraphic interpretations, largely lacking geochronology and whole-rock geochemistry, are given in Beggs et al. (1990) and Cook et al. (1999). Two exploration wells reached basement in the Solander Basin, Parara-1 and Solander-1 (I. M. Turnbull et al., 1993) and are also considered here. Hoiho-1 and Kawau-1 penetrated low-grade metasandstones, interpreted by Beggs et al. (1990) as Buller Terrane, Western Province. We have not examined this material and accept these correlations. Our work focusses on granitoid samples from the boreholes.

Parara-1 cuttings are mostly consistent with derivation from a medium-coarse grained biotite granite. Some fragments appear brecciated and silicified. A single cutting fragment shows granite in contact with silty sandstone, and two fragments comprise fine grained meta-quartz diorite, one with abundant fresh green hornblende and coarse titanite. We interpret this sample to contain minor downhole cavings, rather than representing a proximal sedimentary rock or a granite containing dioritic xenoliths. Solander-1 core comprises fractured, fine grained (1–2 mm) massive biotite granodiorite. Carbonate and zeolite veins are common as is pyrite and patchy greenish alteration of plagioclase. Variation in grainsize may be due to fracturing but also hint at sedimentary matrix; this rock may represent a proximal sediment but is likely to be a reasonable representation of local basement. Pakaha-1 basement cuttings indicate a two-mica granite, with grain size of  $\geq 5$  mm. K-feldspar is characterized by abundant small plagioclase inclusions, mostly euhedral laths, often aligned parallel to grain margins. Plagioclase is generally sericitized; quartz exhibits some deformation. Sharply angular Pukaki-1 cuttings indicate a relatively fresh, olive/brown biotite granite, with several cuttings of brecciated, altered and silicified granite.

SHRIMP U-Pb zircon age data are reported in supporting information Table S2 and shown in Figure 8. P57234 from Parara-1 is dominated by zircons of Carboniferous age, and 8/12 grains give a weighted

**Table 1**

Whole Rock X-Ray Fluorescence Chemical Analyses and Magnetic Susceptibility Measurements of Samples From South Zealandia

Traps	Pukaki-1	Pakaha-1	Parara-1	Solander-1	vSnares Is	Aucklnd Is	Colbeck	Colbeck
P62424	P57236	P57235	P57234	P51537	R10701	OU21583	SID-D2-2	SID-D2-47
Reef	Ct3521m	Ct3360m	Ct3799m	Cr2013m	Outcrop	Outcrop	Dredge	Dredge
Grt	Bt grt	Bt mu grt	Bt grt/sed	Bt gdior	Grt	Bt grt	Grt	Grt
SiO <sub>2</sub>	72.67	72.73	75.82	71.78	64.48	74.14	76.79	77.22
TiO <sub>2</sub>	0.29	0.12	0.14	0.23	0.59	0.07	0.17	0.20
Al <sub>2</sub> O <sub>3</sub>	14.14	14.39	13.34	15.01	18.2	14.39	12.12	11.54
Fe <sub>2</sub> O <sub>3</sub>	1.85	0.91	0.96	1.6	3.33	0.77	1.38	2.12
MnO	0.05	0.02	0.01	0.03	0.04	0.02	0.02	0.02
MgO	0.54	0.23	0.13	0.51	1.31	0.14	0.22	0.08
CaO	1.15	1.13	0.41	1.68	3.56	0.56	0.44	1.14
Na <sub>2</sub> O	4.32	4.13	2.55	4.70	5.74	3.32	3.51	2.17
K <sub>2</sub> O	4.20	4.16	6.01	3.35	2.05	5.29	4.37	5.02
P <sub>2</sub> O <sub>5</sub>	0.11	0.07	0.11	0.08	0.24	0.28	0.05	0.06
LOI	0.62	2.23	0.68	1.21	0.53	0.91	0.72	
Total	99.94	100.12	100.16	100.18	100.07	99.90	99.79	99.57
Ba	529	1,365	929	1,281	9	277	85	339
Ce	68	32	50	30	28	13	106	246
Cr	7	5	3	10	4	<1	2	4
Cu	1	6	3	30	44	<1	4	6
Ga	21	14	14	16	23	24	15	19
La	36	15	22	12	15	8	40	137
Nb	19	3	9	5	5	19	16	19
Ni	1	1	4	3	5	2	3	9
Pb	23	26	30	27	15	34	35	29
Rb	194	109	296	88	63	282	232	213
Sc	6	bd	2	3	4	3	8	3
Sr	205	426	117	570	1,260	87	82	81
Th	11	6	14	6	3	3	42	37
U	1	3	2	bd	0	4	4	32
V	22	10	9	22	68	3	12	10
Y	22	4	9	5	5	11	35	31
Zn	48	45	62	118	58	41	65	41
Zr	188	98	125	108	145	45	116	209
Mag.Sus.	96	15	3	55	600–1,000	<5		243

Note. X-ray fluorescence analyses by Spectracem Analytical, CRL, Lower Hutt, except Colbeck samples (Oregon State University). Mag. Sus. = magnetic susceptibility as dimensionless units  $\times 10^{-5}$  (adjusted for sample size) using GeoInstruments JH-8 meter. Grt = granite; gdior = granodiorite; bt = biotite; mu = muscovite; metased = metasedimentary protolith; trachand = trachyandesite; Ct = cuttings; Cr = core; Pl = Platform; Is = Island(s).

mean age of  $355.6 \pm 6.4$  Ma (MSWD = 1.0; Figure 8a). We interpret the two ~100-Ma grains to have likely been derived from the minor mafic plutonic detritus noted in the cuttings. The bimodal ages affirm the petrographic observations that the cuttings are multilithic, either caved from higher in the borehole, or less likely that the sample represents a sandstone deposited on basement. The weighted mean age of 11/14 zircons from P57235 (Pakaha-1) is  $323.2 \pm 8.5$  Ma (MSWD = 3.4) and from 7/13 zircons from P57236 (Pukaki-1) is  $107.2 \pm 2.6$  Ma (MSWD = 6.0); Figures 8b and 8c). Both samples show minor Carboniferous inheritance; that in Pukaki-1 is consistent with being inherited from granite similar to Pakaha-1 basement, as well as young (123 Ma) inheritance from slightly older Separation Point Suite.

Parara-1 geochemistry is adakitic (Table 1) and together with its Early Carboniferous age (356 Ma) is suggestive of association with Paringa Suite (Tulloch, Ramezani, Kimbrough, et al., 2009), although the geochemistry is likely affected to some degree by downhole cavings, or possibly sedimentary mixing. Solander-1 has a strong adakitic signature (Table 1), and although it has not been dated, this geochemical character is strongly indicative of association with the Early Cretaceous Separation Point Suite. Foley et al. (2013) report major element analyses from Petlab for both Solander-1 and Parara-1, but they have analyzed trace elements by ICPMS. However, these new analyses have low Zr contents compared with the XRF analyses in our original analyses (Table 1) suggesting incomplete digestion of their samples. Two-mica granite from Pakaha-1 (323 Ma) represents Carboniferous basement to the Median Batholith (Tulloch, Ramezani, Kimbrough,

**Table 1** (continued)

Antipodes	Antipodes	Bounty Is	Bounty Is	Bounty Is	Bounty Pl	Bounty Pl	Bounty Pl	Pitt Is
P51539	OU83332	R6180	P28371	P28372	P51222	R6018A	R6018J	P87088
Xenolith	Xenolith	Outcrop	Outcrop	Outcrop	Dredge	Dredge	Dredge	Outcrop
Grt	Gdior	Bt grt	Bt grt	Bt grt	Bt grt	Metased	Metased	Trachyand.
SiO <sub>2</sub>	72.84	64.08	73.59	74.72	72.17	74.66	65.91	62.79
TiO <sub>2</sub>	0.16	0.85	0.17	0.23	0.24	0.18	0.76	0.53
Al <sub>2</sub> O <sub>3</sub>	14.05	18.64	14.03	13.26	14.52	13.33	14.28	11.69
Fe <sub>2</sub> O <sub>3</sub>	1.22	3.27	1.57	1.5	2.28	1.44	6.99	4.92
MnO	0.02	0.05		0.02	0.05	0.02	0.08	0.08
MgO	0.45	0.91	0.37	0.43	0.59	0.43	2.82	2.18
CaO	1.22	3.94	1.55	0.1	1.61	0.82	0.8	5.93
Na <sub>2</sub> O	3.59	4.82	3.74	3.3	3.81	3.12	2.19	1.3
K <sub>2</sub> O	4.8	1.27	3.71	4.04	3.98	5.16	2.43	2.72
P <sub>2</sub> O <sub>5</sub>	0.08	0.2	0.07	0.2	0.1	0.07	0.27	0.12
LOI	1.81	1.11	0.48	1.09	0.6	0.62	3.2	7.13
Total	100.24	99.13	99.32	98.89	99.95	99.85	99.73	99.38
Ba	518	182	503	528	630	294	490	581
Ce	29	52	39	43	43	30	132	61
Cr	<1	6	<1	2	3	<1	64	61
Cu	3	1	<1	3	2	3	68	22
Ga	18	21	16	18	20	16	16	16
La	17	25	20	27	22	16	35	27
Nb	2	10	9	12	13	6	16	11
Ni	<1	2	1	2	3	2	49	21
Pb	31	23	31	32	29	28	86	18
Rb	182	72	151	182	190	189	112	133
Sc	1	10	5	3	4	2	15	8
Sr	198	406	173	155	184	160	122	319
Th	21	13	13	14	16	18	14	14
U	7	4	3	4	3	8	4	6
V	13	71	14	18	22	19	76	153
Y	4	20	13	18	23	28	36	25
Zn	27	62	31	31	45	22	96	87
Zr	117	266	107	119	126	104	168	106
Mag.Sus.	70	15	<10	<10	<10	<10	<5	<5
								1180

et al., 2009), but its highly fractionated nature does not provide a clear suite affinity. Pukaki-1 granite (107 Ma) is a high Sr/Y weakly peraluminous I-type granite (Figures 5c, 5d, and 6g) and, therefore, can be confidently correlated with the Separation Point Suite based on chemistry (supported by age).

### 2.3. Snares and Auckland Islands Granites

Snares Islands are almost entirely composed of variably foliated high-silica muscovite granites. A ductile, mylonitic foliation is developed locally (Scott et al., 2015). The ENE alignment of the Western Chain islets of the Snares Islands with the Sisters Shear Zone of Stewart Island hints at broadly coeval and related extensional exhumation (cf. Kula et al., 2007), but a major linking structure remains to be proven. The geology of the islands, including an overview of previous work, has been summarized by Scott et al. (2015). The geology of the Auckland Islands is dominated by Miocene lavas, but a small inlier of granite basement occurs along an ~200 m stretch of coastline on the north side of Musgrave Peninsula (Adams, 1983). A medium-coarse grained massive granite (OU21583) contains subhedral biotite and quartz, together with plagioclase and perthitic K-feldspar. Estimated modes suggest it may be more properly classified as a quartz monzonite.

Previous geochronological work on the Snares granite includes U-Pb zircon ages of  $109 \pm 1.0$  Ma (P63138; Scott et al., 2015) and  $96 \pm 5$  Ma (5 grains from R10701; Adams et al., 2017) for a weakly deformed muscovite granite. We reinterpret the sparse data for sample R10701 given an MSWD of 13 and apparent discordance for one of two younger analyses and suggest an age of  $99.3 \pm 1.3$  Ma, MSWD = 0.5). Denison and Coombs (1977) reported K/Ar ages of 93 and 97 Ma on muscovite from two different samples (recalculated using

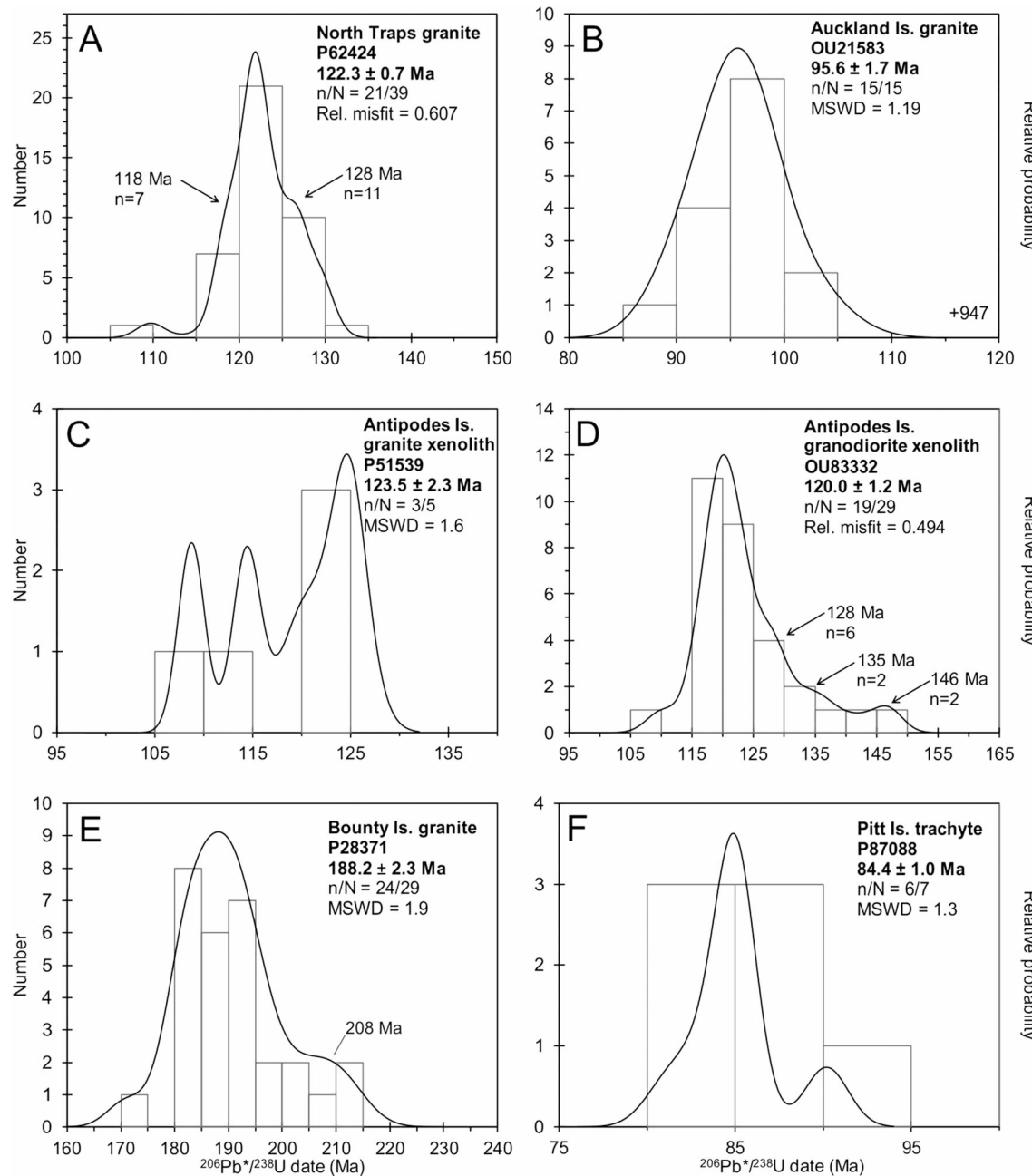


**Figure 4.** Probability plots of zircon ages from Campbell Plateau granitic rocks (a–e) and a Pitt Island trachybasalt (f). Analyses by LA-ICPMS at Otago University's Centre for Trace Element Analysis using Temora-2 calibration standard. n refers to analyses used in age calculation/acceptable analyses (<10% discordant).

current decay constants) and Mortimer et al. (2016) reported a high-quality  $^{40}\text{Ar}/^{39}\text{Ar}$  muscovite isochron age of  $99.5 \pm 0.8$  Ma, which they interpreted as the age at which the sample rapidly cooled through  $350 \pm 50$  °C. From Auckland Island, Adams et al. (2017) reported a  $95 \pm 1$  Ma U-Pb zircon age for granite R24802. K/Ar biotite ages on unaltered samples are as old as 94–97 Ma (Adams, 1983; Denison & Coombs, 1977).

Thirty zircon grains from Auckland Island granite sample OU21583 were analyzed by LA-ICPMS at the University of Otago, but 14 were discarded due to >10% discordance, a result of especially high U contents, and one 947 Ma grain is inherited. The remaining 15 grains (Figure 4b) yield a weighted mean  $^{206}\text{Pb}/^{238}\text{U}$  age of  $95.6 \pm 1.7$  Ma (MSWD = 1.2), within error of the  $95 \pm 1$  Ma age reported by Adams et al. (2017).

**Table 2**  
*Summary of New and Previous Analytical Results From South Zealandia Basement*

Location	Sample	Lithology	Character	Zircon U-Pb	Secondary ages	Whole rock	NZ suite
The Traps	P62424	Bt granite	A/I-type	age (Ma)	(Ma)	$\text{Sr}_i, \varepsilon\text{Nd}_i$	
Pukaki-1	P57236	Bt granite	I-type (adakitic)	$122.3 \pm 0.7$	118, 127, 134	0.7046, -1.9	Rahu
Pakaha-1	P57235	Bt ms granite	Frac S-type?	$107.2 \pm 2.6$	123, 288, circa 300		Separation Point
Parara-1	P57234	Bt granite	I-type (adakitic)	$323.2 \pm 8.5$			Foulwind?
Solander-1	P57237	Bt granodiorite	I-type (adakitic)	$355.6 \pm 6.4$	ca. 100		Paringa
Snares Is	R10701 <sup>a</sup>	Ms granite	Peralum A-type	$95 \pm 1$ (herein $99.3 \pm 1.3$ )			Separation Point
Snares Is	P63138 <sup>a</sup>	Ms granite	Peralum A-type	$109.1 \pm 1.6^a$	ca. 115	0.7010, -7.24	Rahu
Snares Is	OU84689	Hb bt granodiorite	I/S-type	$114.2 \pm 1.2^a$	ca. 121		Rahu
Auckland Is	OU21583	Bt granite	Peralum A-type	$95.6 \pm 1.7$	947	0.70784, -7.3	Horomaka
Antipodes clast	P51539	Bt? granite	I-type	$125.5 \pm 4.1^b$	114–62	0.70513, 1.6	Separation Point?
Antipodes clast	OU83332	Hb bt granodiorite	I-type?	$120.1 \pm 1.2$	128, (135, 146)	0.70582, -0.8	Rahu?
Bounty Is	R6180	Bt granite	I/S-type	$195.3 \pm 3.4$	427–1,103		Darran
Bounty Is	P28371	Bt granite	I/S-type	$188.2 \pm 2.3$	208		Darran
Pitt Island	P87088	Trachyandesite	Benmoreite	$84.4 \pm 1.0$	91		Horomaka

Note. Is = Island(s); Bt = biotite; ms = muscovite; hb = hornblende; Frac = fractionated; Peralum = peraluminous; EK = Early Cretaceous;  $\text{Sr}_i$  = initial  $^{87}\text{Sr}/^{86}\text{Sr}$ ;  $\varepsilon\text{Nd}_i$  = initial  $^{143}\text{Nd}/^{144}\text{Nd}$ .

<sup>a</sup>Scott et al. (2015) and <sup>b</sup>Adams et al. (2017). The age for P28371 is considered the best age for Bounty Island granite. <sup>b</sup>Mean of three methods.

Scott et al. (2015) tentatively concluded that the 109-Ma Snares granite might best be correlated with Rahu Suite of onshore New Zealand. Their concerns about lower Sr and higher Y, Nb, and Rb are amplified here in Figures 5c and 6c. The Al/(Na + K)-Al/(Ca + Na + K) plot (Figure 5e) combined with the flat, relatively heavy REE-enriched and strong negative Eu anomalies (Figure 6g) of both the Snares and Auckland islands samples confirm the distinction from Rahu Suite and suggest a weakly peraluminous A-type signature (e.g., Dahlquist et al., 2010). The 109 Ma Snares granite is coeval with younger plutonism in the Median Batholith (Tarpaulin Suite), whereas the 95 Ma Auckland Island granite postdates the convergent margin batholithic magmatism and can be correlated with some confidence to a pulse of felsic magmatism associated with pre-breakup continental extension (Tulloch, Ramezani, Mortimer, et al., 2009). The interior Gondwana location of these igneous rocks, likely well south of the bulk of the Median Batholith arc, likely explains significant crustal contamination and dilution of the A-type signal in Snares and Auckland islands, a conclusion supported by  $^{87}\text{Sr}/^{86}\text{Sr}_i = 0.7099$  and  $\varepsilon\text{Nd}_i = -7.2$  for the main Snares granite and  $^{87}\text{Sr}/^{86}\text{Sr}_i = 0.7078$  and  $\varepsilon\text{Nd}_i = -7.0$  for the Auckland Islands granite (Figure 7). These enriched  $\varepsilon\text{Nd}_i$  values further emphasize the differences from the Rahu Suite (Waight et al., 1998).

Periodic minor A-type magmatism (Tarpaulin Suite) occurred within Median Batholith, including events at circa 155, 143, 134, 121 Ma, and the 109 Ma (Snares granite, see above) may have resulted from intra-arc or back-arc extension, rather than representing early intraplate extension. The small area of slightly older Broughton Granodiorite (114 Ma, Scott et al., 2015) on Snares Islands may, however, belong to the Rahu Suite. A third Snares age of  $99.3 \pm 1.3$  Ma age (recalculated from Adams et al., 2017) indicates the presence of postsubduction age granitic rocks on Snares Islands.

#### 2.4. Antipodes Island Granite Xenoliths

The Antipodes Island (Figure 1) consist solely of Pleistocene mafic volcanic rocks (Gamble & Adams, 1990; Scott et al., 2013). However, two very rare granitoid xenoliths represent a unique opportunity to infer the nature of the subvolcanic crystalline basement of this part of the Campbell Plateau. Two xenoliths were analyzed for this paper.

Xenolith P51539 is a single friable  $\sim 10 \times 8 \times 4$  cm surrounded, partly melted, grayish-white, xenolith with relict granitic characteristics, showing sharp boundaries with host lava. In thin section (supporting information Figure S2), embayed quartz and feldspar grains up to 2 mm in size are evenly distributed in a vesiculated glass matrix which comprises about 40% of the rock. Remnant mineral grains are quartz (~25%), plagioclase (oligoclase, ~20%), and microcline (~15%). Plagioclase displays normal zoning and twinning, partly obscured by incipient (sericitic?) alteration which also affects microcline. Trace amounts of magnetite are present as

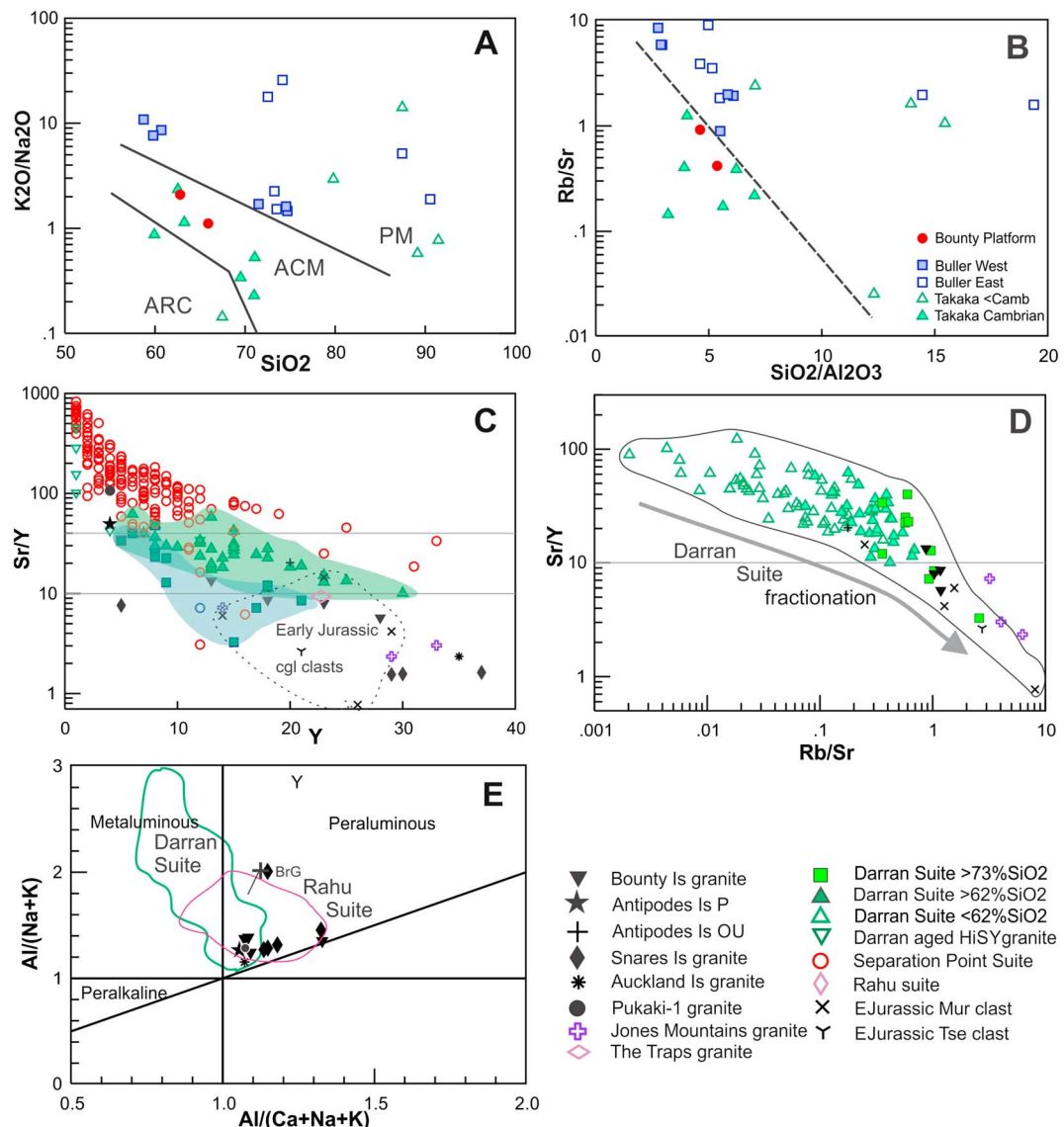


**Figure 5.** Whole-rock geochemistry of Campbell Plateau samples. (a, b) Bounty Platform meta sedimentary compositions. (a) is ARC/ACM/PM classification of Roser et al. (1996). Bounty Platform sandstone compositions best match Cambrian Takaka Terrane. (c, d) Sr/Y versus Y and Rb/Sr plots comparing Campbell Plateau granitic samples to major suites of the Median Batholith. Bounty Island samples are comparable to highly fractionated Darran Suite (pale blue field in (c); lower Sr side of Darran field; green), most commonly observed as Triassic-Jurassic conglomerate clasts. Rahu Suite is mostly confined to Sr/Y < 40, >10. (e) Shand plot showing the weakly peraluminous character of most rocks studied. BrG = Broughton granodiorite, a circa 114 Ma minor component of Snares Islands (Scott et al., 2015). ARC = arc; ACM = active continental margin; PM = passive margin.

scattered grains surrounded by distinctively brown-colored glass; its relatively large size (0.5 mm) and embayed margins suggest that it is also a residual primary phase rather than a later precipitate from the glass. The only hint of primary mafic minerals is a possible phyllosilicate pseudomorph of biotite. Rutile, orthopyroxene, and mullite crystallized from the glass are common but are much finer grained and volumetrically minor (included in the 40% estimate above).

Xenolith OU83332 was a 5 × 4 × 2 cm variably weathered, medium-grained weakly megacrystic granodiorite (grain size 1–3 mm with feldspar megacrysts to 6 mm), and pseudomorphs of amphibole and biotite (supporting information Figure S2). Titanite rhombs have been replaced by leucoxene and traces of rutile. Weakly zoned, albite-twinned plagioclase and biotite both display a moderate igneous foliation.

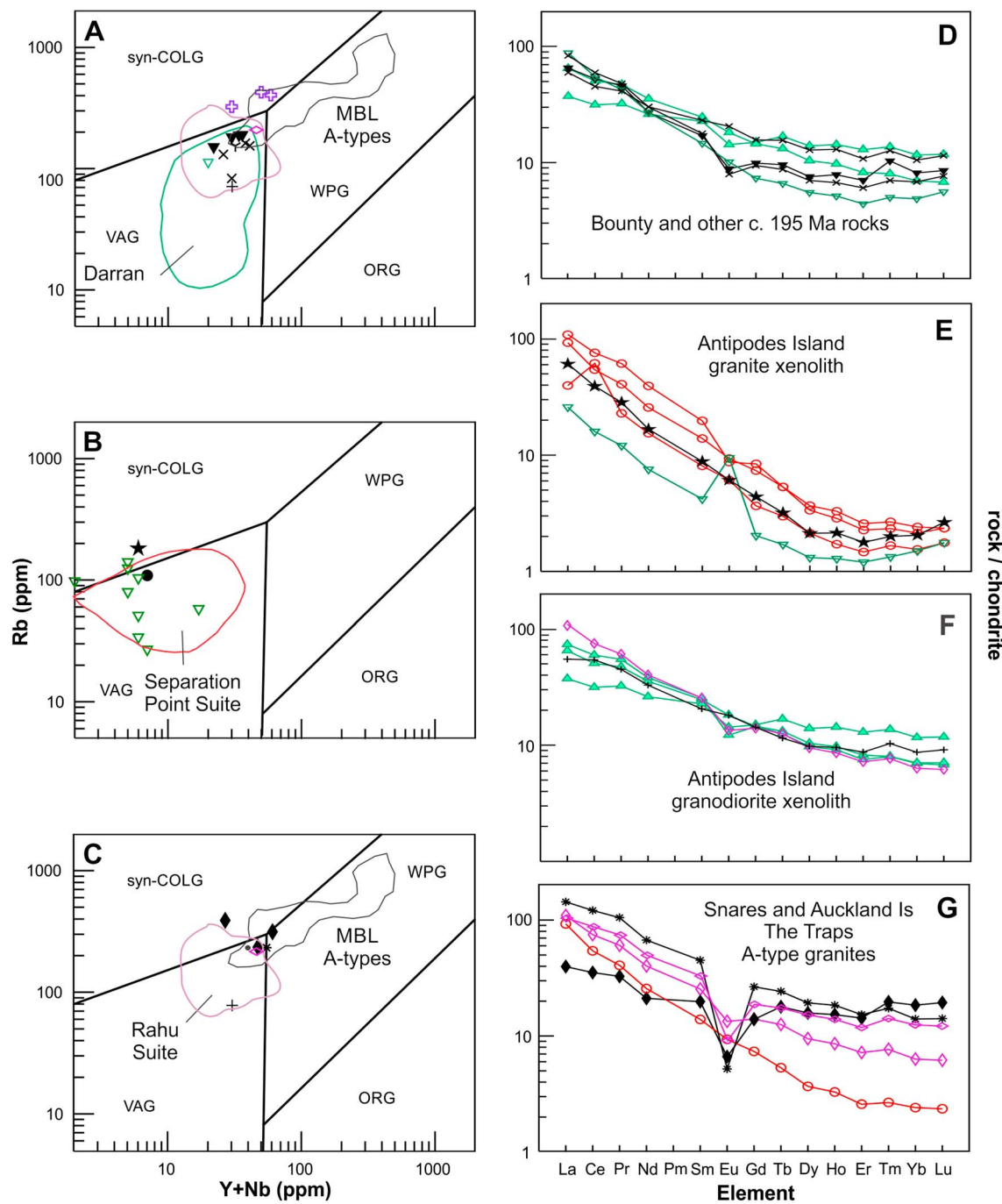


**Figure 6.** (a–c) Rb versus Nb + Y tectonic discrimination plots. (a) Bounty Island granite compared with Darran and Rahu Suites, clasts from Early Jurassic and Early Cretaceous conglomerates in New Zealand, and samples of Jones Mountains granite south of Eight Coast, West Antarctica. (b) Antipodes Island granite xenolith and Pukaki-1 well compared with high Sr/Y rocks in Median Batholith: Separation Point Suite, and uncommon high Sr/Y granites from the Darran Suite. (c) Granites from Auckland and Snares Islands and granodiorite xenolith from Antipodes Island compared with the Rahu Suite, mostly inboard of Median Batholith in New Zealand, and A-type granites from Marie Byrd Land. The latter includes one of two granites from the Colbeck Trough—a black dot to the left of the lowest Rb Snares sample. The other Colbeck sample plots between the aforementioned Snares sample and the Auckland Islands sample. (d–g) Chondrite-normalized (Nakamura, 1974) rare earth element plots comparing Bounty Island granite, Antipodes Island granite, Antipodes Island granite and granodiorite xenoliths, and Bounty Islands granite with Median Batholith plutonic belts of onshore New Zealand (Tulloch & Kimbrough, 2003); dominated by Separation Point and Darran Suites and the inboard Rahu Suite. Symbols as for Figure 5.

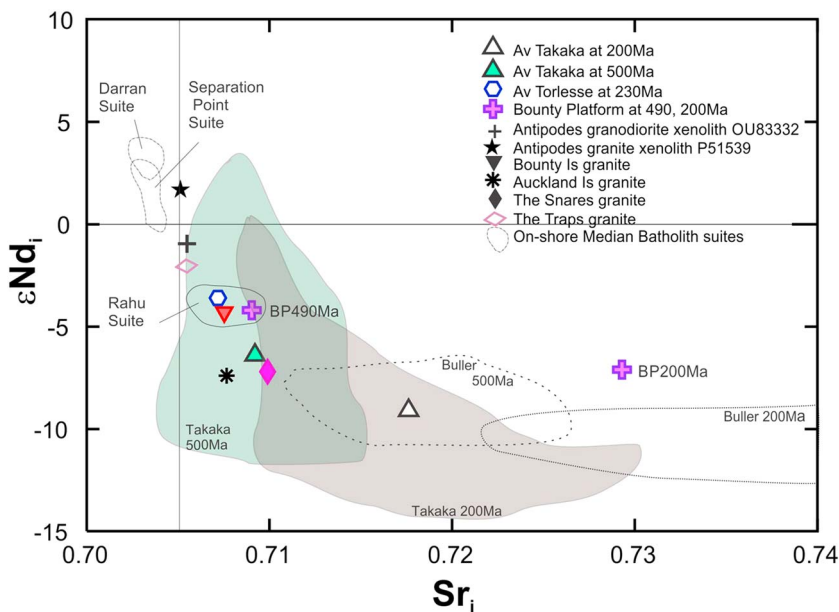


**Figure 7.** Nd and Sr initial isotopic compositions of Antipodes granite xenolith and Bounty Islands granite and metasedimentary rock, compared with onshore New Zealand terranes and batholiths. Antipodes Island granite xenolith is slightly displaced from onshore correlative Separation Point Suite, possibly because of incorporation of a supracrustal component but more likely disturbance of Rb/Sr during partial melting of the xenolith. Bounty Islands granite contains a significant crustal component, as indicated by Paleozoic and Proterozoic inherited zircon. The Bounty Islands metasedimentary rock sample has a composition comparable to the Western Province (Takaka Terrane). At 200 Ma it is far too radiogenic to be compared with the Eastern Province terranes (represented by Average Torlesse). Data for Takaka Terrane: Wombacher and Münker (2000), Greenland Group—Buller Terrane, B: Adams et al. (2005) and Tulloch, Ramezani, Kimbrough, et al., 2009; Median Batholith: Muir et al. (1998) and Tulloch and Kimbrough (2003); Rahu Suite: Waight et al. (1998); Bounty Islands granite: Pickett and Wasserburg (1989); Average Torlesse (Rakaia Terrane recalculated at 200 Ma): Adams et al. (2005). Bounty Islands metasedimentary rock (A713, Cullen, 1975) and Antipodes Island granite xenolith (P51539): this paper (supporting information Table S3). Initial isotope compositions for igneous rocks are calculated at their individual crystallization ages.

Minor patches of yellowish weakly birefringent glass occur, generally in association with altered biotite and amphibole grains. Some parts of OU83332 have a 1–3 mm thick gray rind of vesiculated basalt mingled with melted granodiorite. For whole rock chemistry and zircon separation, ~24 g of unweathered rind-free granodiorite was used. A further 30 g of weathered xenolith was crushed to provide additional zircon.

A mineral separate from granite xenolith sample P51539 yielded 10 zircon crystals, and cathodoluminescence (CL) images of seven of these are shown in supporting information Figure S3. Morphology ranges from multifaceted equant to prismatic, and grains are 40–150  $\mu\text{m}$  long. The zircons exhibit oscillatory zoned CL-bright cores, typically overgrown by CL-dark, high to very high uranium, rims, and patches. Nine analyses of these seven grains were made by SHRIMP-RG (Reverse Geometry) methods at Stanford University, using the AS3 zircon standard. Seven points comprise a cluster with a weighted mean age of  $128.4 \pm 4.8$  Ma (MSWD = 3.6; Figure 8d). Two grains are significantly younger (ca. 123 Ma) and are likely affected by Pb loss. Two even younger (84 and 68 Ma) analyses (not shown in Figure 8) were rejected due to their very high U (592 and 3,521 ppm); the radiation damage most likely also led to major Pb loss and the resultant young ages.

Thermal ionization mass spectrometry (TIMS) single-grain zircon analysis was undertaken on the three remaining grains at Brown University, and the data are presented Figure 9. Although the multifaceted grain is nearly concordant at circa 120 Ma, the prismatic grains exhibit strong to extreme reverse discordance. The three data points form a discordia (MSWD = 0.72) that we suggest has age significance, whereby the upper intercept of  $141 \pm 32$  Ma likely encompasses the crystallization age of the granite. However, we report the more precise  $^{207}\text{Pb}/^{206}\text{Pb}$  age of the near concordant grain as the best TIMS estimation of the primary crystallization age. However, we note that uncertainties in the U decay constant (Schoene et al., 2006) make this

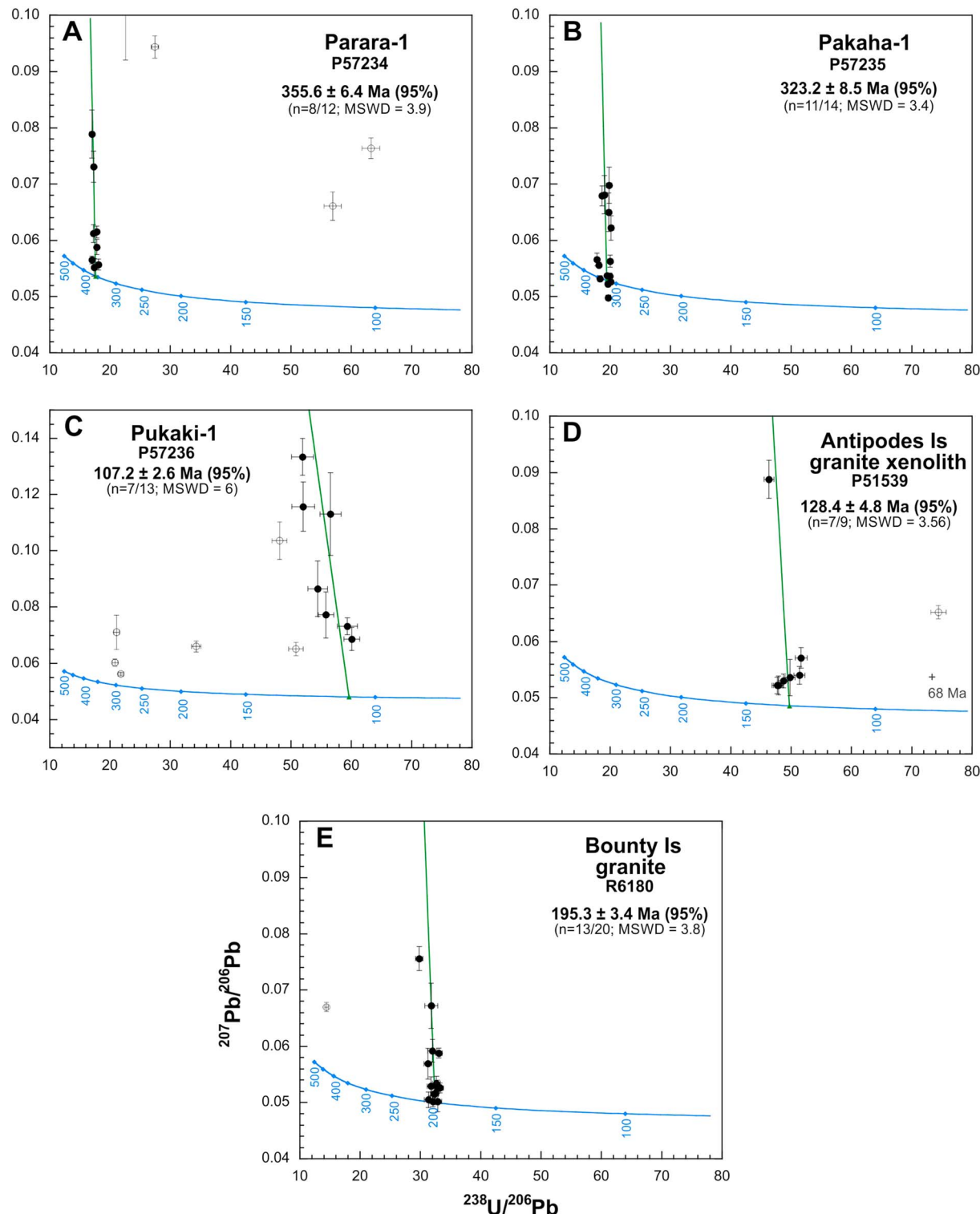


**Figure 8.** Sensitive high-resolution ion microprobe zircon isotopic data plotted on Tera-Wasserburg concordia plots. Reported age is  $^{238}\text{U}/^{206}\text{Pb}$  intercept of discordia anchored in common lead of Broken Hill composition (Muir et al., 1994). (a–c) Great South Basin well cutting samples; (d and e) Samples from Antipodes and Bounty Islands, respectively.

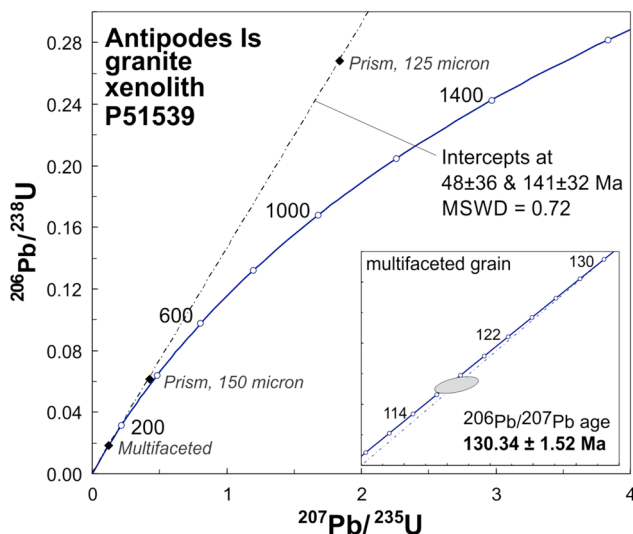


**Figure 9.** Thermal ionization mass spectrometry U-Pb isotopic age results for single zircon grains from Antipodes Island granite xenolith (Table S3). U-Pb concordia plot shows apparent minor and major reverse discordance for two grains. Maximum age of 130 Ma age is based on the  $^{207}\text{Pb}/^{206}\text{Pb}$  age of the near concordant multifaceted grain, but we report a lower age  $^{207}\text{Pb}/^{206}\text{Pb}$  age of 126 Ma based on likely error in decay constants (see text).

The chemical analyses (Tables 1 and 2) for the two xenoliths are quite distinct. Both appear to represent sensible compositions, largely unaffected by their basalt host. Granitic xenolith P51539 has a moderately high Sr/Y = 50 (Figure 5) suggestive of correlation with the Separation Point Suite, despite having a relatively low Sr content. We assume that potential exchange of elements with the basaltic host has not had a major effect other than for large ion lithophile elements. Suite-discriminatory elements REE, Y and Sr would likely be less affected. A chondrite-normalized plot (Figure 6b) shows depleted heavy REE and lacks a Eu anomaly, both consistent with comparison with Separation Point Suite. However, the medium REE (Dy-Tm) are somewhat depleted relative to Yb, Lu, defining a curved pattern suggestive of magmatic amphibole fractionation (Davidson et al., 2007; Macpherson et al., 2006) rather than the residual garnet control attributed to the Separation Point Suite (Muir et al., 1995; Tulloch & Rabone, 1993). In this respect, the REE pattern is similar to minor volumes of weakly high Sr/Y rocks that accompany Darran Suite magmatism (Figures 5b and 6b). However, as Dy = Yb for P51539, and the Eu anomaly is absent, we conclude the pattern is more similar to that of adakitic origin. The circa 124 Ma age is also more consistent with correlation to the adakitic Separation Point Suite of the onshore Median Batholith, than Darran Suite (Allibone & Tulloch, 2004; Tulloch & Kimbrough, 2003). Sr-Nd isotope data with slightly positive  $\epsilon\text{Nd}_i$  (Figure 7) is perhaps more consistent with Separation Point Suite in New Zealand, and on balance we conclude affinity with the adakitic Separation Point Suite rather than Darran Suite is most probable.

Granodiorite xenolith OU83332 has a peraluminous composition (Figure 5e) and low Sr/Y (Figure 5d), both within the range of the Rahu and Darran suites of onshore New Zealand (Tulloch & Kimbrough, 2003; Waight et al., 1998). The zircon U-Pb age of circa 120 Ma is more consistent with the Rahu Suite. However, the rock has higher Na/K than Rahu Suite rocks with similar SiO<sub>2</sub>; Ba = 182 ppm is significantly lower. Possible explanations might be either a “reverse nugget effect” in that the 24 g analyzed sample may have under sampled scattered K-feldspar megacrysts and/or diffusion or devolatilization of K out of the xenolith as shown by visible alteration of biotite (also cf. experiments of Watson & Jurewicz, 1984). We suggest the latter is the most significant mechanism for potential K, Ba, and Rb depletion from an original rock of Rahu Suite composition. A slightly positive Eu anomaly (Figure 6e) might indicate accumulation of plagioclase, perhaps represented by the weak igneous lamination. We conclude that the peraluminous composition and age are most consistent with a Rahu Suite correlation, although Sr-Nd isotopes (Figure 7) are more juvenile than most Rahu Suite. In this respect, this xenolith is similar to approximately coeval granite from The Traps, offshore SE Stewart Island.

a maximum age, and we have recalculated that intercept age down to where the discordia cuts the concordia error boundary ( $126 \pm 1.5$  Ma), rather than concordia, on this basis.

A second separation yielded a further 11 grains that were dated by LA-ICPMS using Temora (locality for standard referred to elsewhere in ms)-2 standard. Of seven acceptably concordant analyses, the oldest three yield a weighted mean age of  $123.5 \pm 2.3$  Ma (MSWD = 1.6, 95% confidence). The other analyses have ages ranging down to 80 Ma, consistent with Pb-loss induced by radiation damage due to their very high U contents (~2,000–5,000 ppm).

In summary, ages from secondary ion mass spectrometry, LA-ICPMS, and single grain TIMS for Antipodes granite sample P51539 overlap at  $125.5 \pm 4.1$  Ma (95% confidence MSWD = 2.5). The high U zones yielded SHRIMP and LA-ICPMS ages ranging from 95 to 63 Ma, reflecting significant Pb-loss.

Granodiorite xenolith sample OU83332 yielded abundant zircon. Of 48 LA-ICPMS analyses, 30 were acceptably concordant (Table S1), but they define a strongly asymmetrical peak skewed to older ages (Figure 4). After excluding a young outlier at 110 Ma we used Gaussian deconvolution to quantify abundant inheritance ranging from 128 to 146 Ma. The main peak was thus determined as  $120.0 \pm 1.2$  Ma from 19 analyses.

## 2.5. Bounty Platform Metasedimentary Rocks

Cullen (1975) described rocks dredged from around the Bounty Islands as low metamorphic grade, fine- to medium-grained litharenites. Quartz was the most abundant sand-sized mineral; oligoclase-albite plagioclase was common, but no K-feldspar was observed in stained thin section. Low-grade muscovite was common and biotite in one sample (A713) might have been of contact metamorphic origin. Cullen (1975) concluded that the high quartz/feldspar was indicative of a Western Province origin, probably from the Greenland Group (Buller Terrane).

New petrographic data on three metasedimentary rocks from stations A704 (samples R6018A and J), and A713 (sample R6019) are provided here as context for new analyses, reported below. R6018A shows microbedding between coarse and fine-grained sandstones, and metamorphic mica (~40  $\mu\text{m}$ ) orientations are random, suggestive of a contact metamorphic origin. The coarser grained part is recrystallized and shows no sedimentary grain boundaries. R6018J is a sandy, calcareous mudstone. It has chlorite porphyroblasts up to 200  $\mu\text{m}$  in size (possibly after biotite) and patches of secondary carbonate up to 200  $\mu\text{m}$ . R6019 contains polycrystalline aggregates of quartz up to 200  $\mu\text{m}$  in size; if these are clastic relicts, they would be fine sand size; metamorphic biotite occurs in the matrix and as ~100- $\mu\text{m}$  porphyroblasts. R6019 has a weak penetrative cleavage.

The petrography of the three samples indicates a Western Province (either Buller or Takaka Terrane) correlation. Adams and Cullen (1978) reported a 228 Ma K/Ar total rock age for argillite at station A704. For a sandstone from the same station, Adams (2008) reported two single grain detrital U-Pb ages of  $482 \pm 5$  Ma and  $1,230 \pm 31$  Ma. Rb-Sr dating of micaeous flakes yielded a (metamorphic) isochron age of  $174 \pm 32$  Ma. Laser fusion  $^{39}\text{Ar}/^{40}\text{Ar}$  ages on sericitic flakes from two separate stations yielded mean (metamorphic) ages of  $232 \pm 4$  Ma and  $182 \pm 3$  Ma. Adams et al. (2005) reported an  $^{87}\text{Sr}/^{86}\text{Sr}_i$  of 0.70995 and  $\epsilon\text{Nd}_i$  of  $-8.3$  (both calculated at 414 Ma) for a Bounty metasedimentary sample. These analytical data also indicate a Western Province metasedimentary correlation.

Major element compositions of two metasedimentary rocks from Station A704, ~35 km east of the Bounty Islands, are compared with the Buller-Takaka Terrane data set of Roser et al. (1996) in Figures 5a and 5b. Satisfactory comparison with Western Province terranes is very dependent on knowledge of grain size, information for which is not entirely clear in the Bounty Platform samples. Possibly the Bounty samples match better with the Cambrian (active continental margin) part of the Takaka Terrane, rather than either post-Cambrian Takaka Terrane or Buller Terrane (both passive margin), although this is not obviously supported by analysis of a single detrital zircon from Station 704 that yielded an age of  $482 \pm 5$  Ma. The Bounty Platform metasedimentary rocks also overlap Mesozoic Torlesse Terrane, but the presence of Early Paleozoic and Precambrian (and essential absence of Mesozoic) inherited zircon in Bounty Island granite (below) supports an Early Paleozoic depositional age for these metasedimentary rocks. Initial Sr and Nd isotope ratios for one sample (Table S3) are compared with Early Paleozoic and Mesozoic greywackes from New Zealand in Figure 7. As with the whole rock geochemistry, a Western, rather than Eastern Province correlation is supported.

## 2.6. Bounty Islands Granite

The 15 or so barren islets that comprise Bounty Islands total slightly less than 1  $\text{km}^2$  in area, with the largest ~400 m across (supporting information Figure S4). The islands are composed of relatively homogeneous medium-grained, equigranular to inequigranular massive biotite granite, that contains inclusions of amphibolite (Cullen, 1975). Wasserburg et al. (1963) reported a modal analysis of a granite as ~32% quartz, 41% plagioclase, 21% K-feldspar, and 6% biotite; traces of muscovite, clinzoisite and opaque grains are likely secondary. Magnetic susceptibility measurements (Table 1) on seven granite samples indicate the essential absence of magnetite. Sample R6180 is weakly megacrystic with K-feldspar megacrysts up to 12 mm long, as well as plagioclase and quartz (6 mm) and biotite (2 mm). Granites, along with quartz-feldspar porphyries, microtonalites and microdiorites have been dredged from 11 sites on the Bounty Platform, up to 15 km east and 25 km west of the islands (Cullen, 1975).

Previous analytical work on Bounty Islands granites includes K/Ar dating, the oldest biotite ages being 192 and 193 Ma (Wasserburg et al., 1963; Adams & Cullen, 1978; recalculated here with current decay constants). Adams et al. (2017) reported a LA-ICPMS U-Pb zircon age of  $191 \pm 2$  Ma (with one 427-Ma

inherited grain). Pickett and Wasserburg (1989) reported  $^{87}\text{Sr}/^{86}\text{Sr}_i = 0.7082$ , and  $\epsilon\text{Nd}_i = -4.4$ . Adams (1985) reported K/Ar whole rock ages of circa 140, 157 and 186 Ma, for three east-west striking basalt dikes that cut the granite. Mortimer et al. (2015) reported weighted mean zircon and apatite fission track ages of  $105 \pm 8$  Ma and  $80 \pm 6$  Ma, respectively, for Bounty Islands granite.

Nineteen analyses on 17 grains were determined on sample R6180 (from the summit of Tunnel Island) using SHRIMP I at ANU (AS3 zircon standard). Fourteen analyses form a coherent group, interpreted as the crystallization age, at  $195.3 \pm 3.4$  Ma ( $2\sigma$ , MSWD = 3.8, Figure 8e). Note that this is the same sample and result referred to as “Ireland (pers. comm.)” in Wandres et al. (2004). The remaining five analyses range in age from 423 and 926–1060 Ma and represent inherited components, consistent with derivation from nearby dredged low-grade metasedimentary rocks of New Zealand’s Western Province (Adams, 2008; Adams & Cullen 1978).

A second sample (P28371, assumed to come from Depot Island) was dated by LA-ICPMS. Forty-one grains were analyzed (supporting information Table S2), of which 29 were satisfactorily concordant and are plotted on Figure 4e. Four ages significantly older than the main peak give an error-weighted mean of  $208 \pm 5$  Ma and are considered to be inherited. The remaining 24 grains have a weighted mean age of  $188.2 \pm 2.3$  Ma (MSWD = 1.9). This age is similar to the Adams et al. (2017) age of  $191 \pm 2$  Ma but is significantly younger than the SHRIMP age of  $196 \pm 3.4$  Ma. These three ages might suggest that plutonic bodies ranging in age from 196 to 188 Ma are present on Bounty Islands, but as we cannot rule out issues related to the AS3 calibration standard (Schmitz et al., 2003), we consider the LA-ICPMS age of  $188.2 \pm 2.3$  Ma to be the best estimate of the age of Bounty Islands Granite. Triassic K/Ar ages of dredged Bounty Platform metamorphic rocks (Adams, 2008; Adams & Cullen, 1978) suggest that early Late Triassic plutons, which have metamorphosed country rock, are also present nearby on the Bounty Platform, in addition to the latest Late Triassic zircon inheritance in our 188 Ma sample from the Bounty Islands. Together, this pattern matches well the Darran Suite age pattern onshore.

Whole rock XRF analyses of four samples of Bounty Islands biotite granite in a strict sense are presented in Tables 1 and 2. On a Shand plot (Figure 5e) they are compared with the 230–135 Ma Darran Suite, the major Mesozoic subduction-related igneous suite of on-land New Zealand. Three out of four Bounty samples lie within the peraluminous, most evolved, part of the Darran Suite field on the Shand plot. All samples also lie within the most evolved end of the Darran suite field on a Rb versus Nb + Y plot (Pearce et al., 1984; Figure 6a). However, all Bounty Islands samples form a distinct trend below the lower boundary of the Darran Suite field on a Sr/Y versus Y plot (Figure 5c). The Sr-Nd isotopic composition of Bounty Islands granite ( $^{87}\text{Sr}/^{86}\text{Sr}_i = 0.70754$ ,  $\epsilon\text{Nd}_i = -4.3$ , recalculated at 188 Ma from Pickett & Wasserburg, 1989) is quite distinct from its Darran Suite onshore general age equivalent, although this composition is not inconsistent with simple binary mixing of Darran and Takaka Terrane metasedimentary compositions (Figure 7). Assimilation of metasedimentary rock of R6018A composition could also explain low Sr/Y in Bounty Islands granite, especially as there is considerable dispersion of Bounty Islands granite compositions toward R6018A (Figure 5c).

## 2.7. Pitt Island Trachyte

Pitt Island, SE of Chatham Island, is dominated by Late Cretaceous volcanic and sedimentary rocks (Campbell et al., 1993). A graben containing early Late Cretaceous Waihere Bay Group sedimentary rocks, is defined by ENE-trending faults that parallel graben structures identified in offshore seismic studies (Wood & Anderson, 1989). Most volcanic rocks are basaltic (Panter et al., 2006), but a sample from a trachyte dyke swarm striking 160–172° in the SW of the island (supporting information Figure S5) was collected for zircon geochronology. In thin section, P87088 is porphyritic with ~6% plagioclase phenocrysts (3–4 mm), set in a strongly trachytic groundmass dominated by plagioclase laths (~0.3 mm) with interstitial brown hornblende and accessory magnetite.

All seven zircon grains from P87088 analyzed by LA-ICPMS are acceptably concordant. After discounting an outlier at 90 Ma, the remaining six grains yield a weighted mean age of  $84.3 \pm 0.9$  Ma (MSWD = 1.4; Figure 4f). The 84 Ma age lies within the reported 85–82 Ma age range of Pitt and Chatham islands intraplate lavas dated using  $^{40}\text{Ar}/^{39}\text{Ar}$  of plagioclase and hornblende by Panter et al. (2006). As an aside, baddeleyite is also present in P87088 and contains 20,000–30,000 ppm U. Use of a baddeleyite standard (outside the scope

of this paper) would likely provide highly precise ages. Dyke sample P87088 has a trachyandesitic composition; relatively high  $\text{Na}_2\text{O}/\text{K}_2\text{O}$  indicates a marginally benmoritic classification.

### 2.8. Colbeck Trough, West Antarctica

Mylonitic Byrd Coast granite samples dredged from the Colbeck Trough were described in Siddoway et al. (2004). Cooling ages of 98–95 Ma ( $^{40}\text{Ar}/^{39}\text{Ar}$  biotite and K-feldspar) were reported, providing an age of extensional exhumation. Here we report whole-rock geochemical analyses of the granite to complement our granite data set from South Zealandia (Tables 1, 2). These analyses overlap both the 109 Ma Snares and circa 96 Ma Auckland Island granite, and the low-Rb end of Byrd Coast granite distribution from Marie Byrd Land in Figure 6.

## 3. Geophysical Results

### 3.1. CMAS

Since its discovery by Davey and Christoffel (1978), the CMAS has been regarded as a representing a major, basement-controlled feature. The CMAS has persisted in successive regional magnetic data sets and their derivative grids (e.g., Frogtech, 2013; Sutherland, 1999) through to the version used in Figure 2. Below, we present a qualitative interpretation of the CMAS, and the gravity map (Figure 3).

The predominant and major area of positive anomalies covers ~20% of the Campbell Plateau and extends ~600 km WSW-ENE from near Auckland Island to the Bounty Platform where the anomalies become more fragmented. In this latest magnetic data set, two spatial trends are evident, a predominant WSW-ENE alignment of positive anomalies and a subordinate, orthogonal NNW-SSE alignment. Many smaller isolated positive magnetic anomalies are also present, especially in the southern half of the Campbell Plateau, in which these two trends are also visible. A set of gravity anomaly lineations parallel the main WSW-ENE magnetic anomaly (Sandwell & Smith, 1997; Sutherland, 1999).

Notably, the NNW-striking alignments of the CMAS are parallel to the Antipodes, Bollons, Pahemo, Kohiku, and Emerald fracture zones in the Southern Ocean, as well as the 89- to 80-Ma stretching lineations and transfer faults in the Sisters Shear Zone (Kula et al., 2007; Figure 12). The WSW-striking alignments of the CMAS are parallel to mid ocean ridge magnetic anomalies, and lineaments in the fault-controlled Great South, Pukaki, and Outer Campbell basins. Such parallelism suggests that the source of the CMAS is associated with rifting, rather than a prerift basement feature.

There are three lines of supporting evidence for a rift origin of the CMAS: (1) Much of the onshore Median Batholith has negligible magnetic expression, with the relatively minor exceptions of Darran and Rotoroa Complexes (Figure 2). For example, the largest plutons that comprise much of western Fiordland (Allibone et al., 2009) represent exhumed lower crust and are associated with little or no magnetic anomaly. (2) In a geophysical profile, Grobys et al. (2009) invoked underplating and shallow crustal dike-like features beneath the central Campbell Plateau to explain individual magnetic anomalies within the CMAS. (3) In eastern Chatham Rise, similar, but smaller magnetic anomalies are present (Figures 2 and 12). Like those in the CMAS, WSW-ENE and NNW-SSE alignments are visible. In particular, three parallel positive anomalies ~250 km long, south of the Chatham Islands, strike WSW-ENE. The northwesternmost of these anomalies encompasses Pitt Island (the only island within the CMAS) and is parallel to nearby ENE-trending grabens (Wood & Anderson, 1989). At least half of Pitt Island is composed of Late Cretaceous Southern Volcanics (Campbell et al., 1993), and the 84 Ma Pitt Island trachyte dated in this paper was sampled from a SSE-striking dike swarm that parallels the Antipodes and Udintsev fracture zones.

### 3.2. Seismic Reflection Profiles

Acoustic basement is imaged in many research and industry seismic reflection profiles in Canterbury and Great South sedimentary basins (e.g., Cook et al., 1999). For the most part, acoustic basement is isotropic. However, some gently dipping, intrabasement reflectors were interpreted as Haast Schist foliation and Murihiku Terrane bedding by Mortimer et al. (2002). Based on recent industry seismic compilations, we are now able to map out the lateral extent of intrabasement reflectivity in Canterbury and Great South basins (Figures 10 and 11). The large, northern area of basement reflectivity in Figure 10 lies offshore from Torlesse terrane greywacke and schist. Reflectors are strong, but laterally discontinuous and possibly imbricated

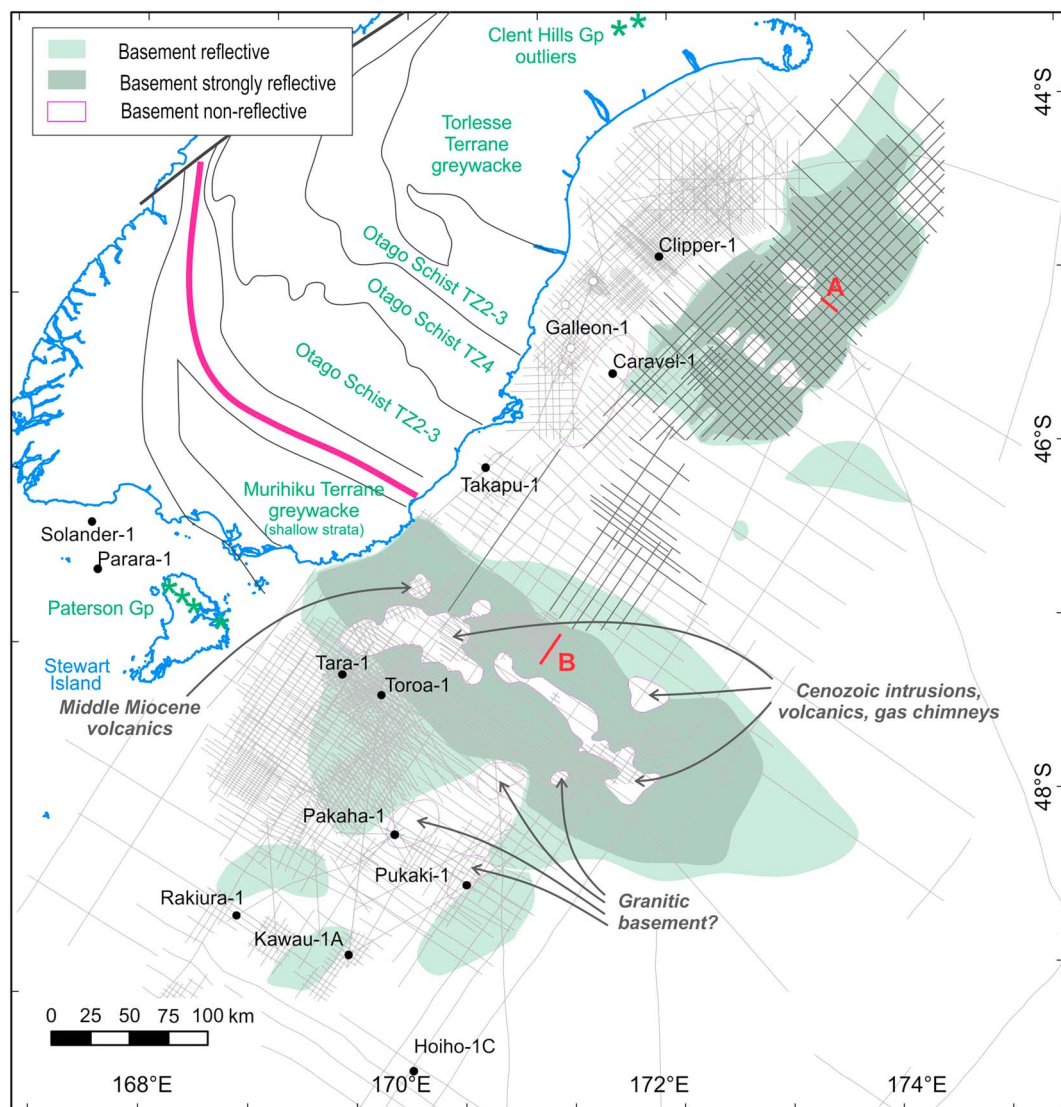


**Figure 10.** Map showing seismic data coverage and interpretation for Great South and Canterbury basins. A and B refer to seismic sections in Figure 11. Inferred offshore extent of Murihiku Terrane and seismically recognizable patches of granitic basement are shown, as are Cenozoic volcanic rocks (\*) that may be contributing to the Stokes Magnetic Anomaly System. Bright pink line is Dun Mountain Ophiolite Belt.

(Figure 11a). Our preferred interpretation is that, in large part, it represents subhorizontal Otago Schist basement. As such it helps define the subbasin interpolated extent of schist between Otago and the Chatham Islands. Another possibility is that it represents deformed, but gently dipping Torlesse trench-slope basins akin to the Clent Hills Group strata seen as small outliers in Canterbury (Figure 10) or, even less likely, large areas of subhorizontally bedded Torlesse greywacke.

The large, southern area of basement reflectivity lies offshore from the projected extent of the subhorizontally dipping Murihiku Terrane (Bache et al., 2014). Basement reflectors are thin but continuous over tens of kilometer, and are truncated by the basement cover unconformity (Figure 11b). We are moderately confident that most of the highly reflective southern region in Figure 10 corresponds to Murihiku Terrane and that the syncline axis in Figure 11b is the Southland Syncline. Regions of weaker but still visible reflectivity SE of Stewart Island are not along strike from known on land Murihiku Terrane (Figure 10). Their origin is unclear but they may correspond to outliers of Jurassic Paterson Group (Allibone & Tulloch, 2004, 2008) or other Early Mesozoic volcano-sedimentary units related to Median Batholith magmatism.

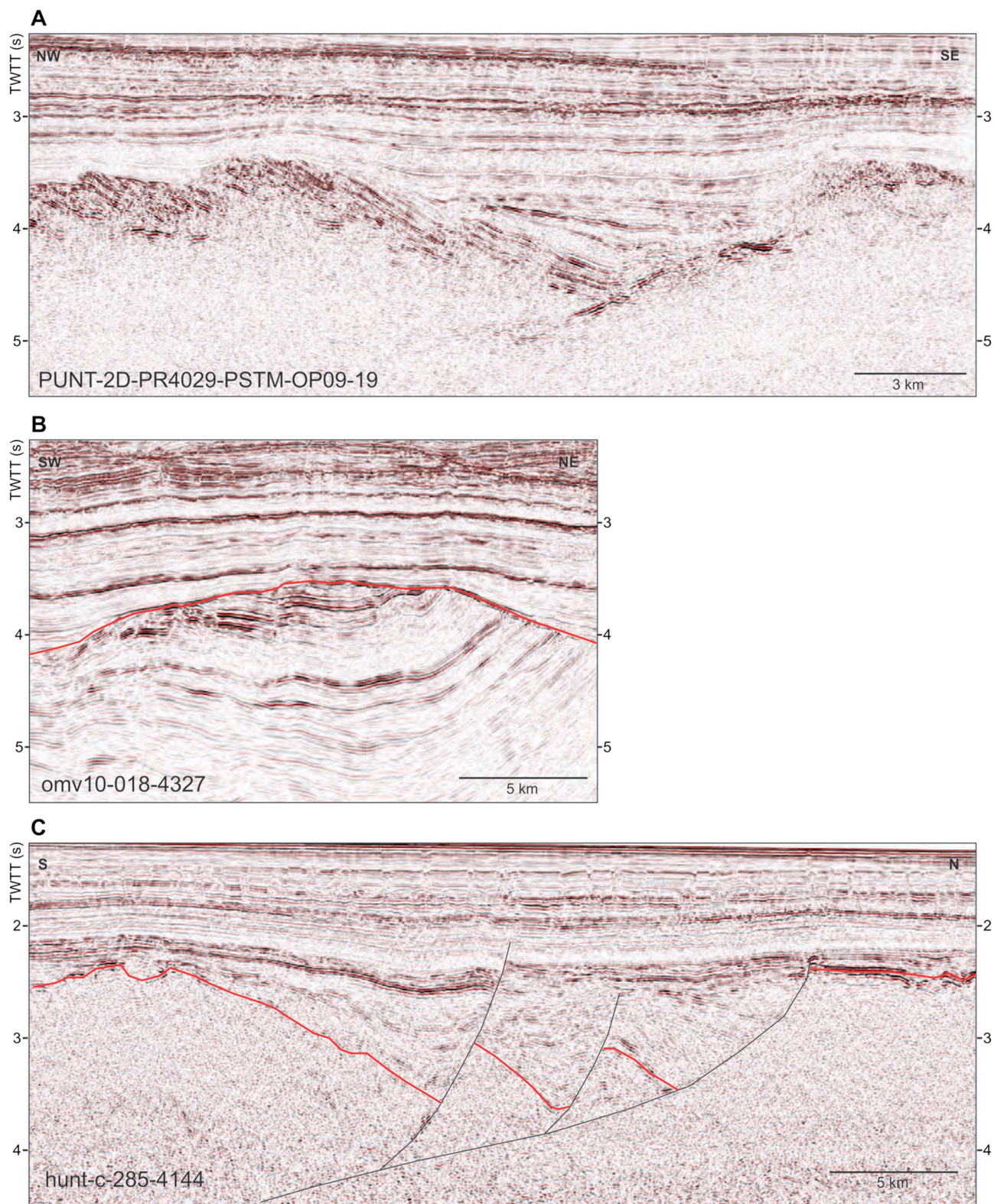


**Figure 11.** Seismic sections from locations in western South Zealandia. (a) Offshore from Torlesse Terrane greywacke and schist. Strong, possibly imbricated, reflectors likely represent subhorizontal schist basement. (b) Offshore Murihiku Terrane showing probable eastward continuation of the Southland Syncline. (c) Seismic section SE of Auckland Island (Figures 2 and 10). Grabens controlled by south dipping normal faults offset basement. Juxtaposition of dense basement and less dense rift basin strata likely produces the associated gravity lineaments.

We also present an interpretation of a seismic reflection profile on the southwestern Campbell Plateau (Figures 1, 3, and 11c). Hunt profile C285 lies SE of the Auckland Islands and crosses some prominent gravity lineations (Figure 3). Interpretation of this line reveals three adjacent grabens controlled by south dipping faults that offset basement. It is these rift structures that presumably create the gravity lineaments through the juxtaposition of a dense basement footwall adjacent to lower density synrift strata. Within each graben, fanning reflectors indicates growth strata during normal faulting. Speculatively, the faults are listric and sole into a subhorizontal crustal detachment ~7 km below the seafloor. On this basis, palinspastic restoration of the faults requires ~8 km of extension along the 48-km-long line ( $\beta = 1.2$ ).

## 4. Discussion

### 4.1. Onland-Offshore Correlations

Our new geological and geophysical data and interpretations, outlined above, can be used to test various extrapolations of onland geological units across the Campbell Plateau. The key suite and terrane correlations are summarized in Table 2. In turn, these can be used to track the spatial extent of the batholiths and terranes. Invariably this is a less confident exercise inasmuch as (a) it is not known how representative are the individual samples analyzed, (b) there are large distances between samples, and (c) in principle, igneous suites are not necessarily restricted to batholithic belts (Tulloch, 1988). Nonetheless, because the Darran and Separation Point Suites are largely restricted to Median Batholith (Mortimer et al., 1999; Tulloch & Kimbrough, 2003), the Pukaki-1, Bounty, and Antipodes samples support the notion that the Median Batholith extrapolates east to the Bounty Platform and intrudes Takaka Terrane near.

*Bounty Island.* The Early Jurassic Bounty Islands sample and Early Cretaceous Antipodes Island samples match the arc-normal age progression seen in Median Batholith onland (younger ages/adakitic plutons to the south and west).

Torlesse and Caples terrane Haast Schist occurrences on Chatham Islands and Stuttgart seamount (Mortimer et al., 2006) also indicate long-baseline east-west strikes to the basement structural grain and thus support the extrapolated trend of the Median Batholith. Some intrabasement reflectivity in the Canterbury Basin (Figure 11a) may also track the extent of flat-lying Haast Schist core rocks between the Otago Coast and Chatham Islands.

The distance between the Bounty and Antipodes Island is ~220 km. This is greater than the width of the onland Median Batholith (maximum ~75 km for both Fiordland and Stewart Island) and raises the question as to whether contiguous plutonic rocks (the batholith) span the entire distance between the islands or if, say, samples from one or both of the islands are from satellite plutons outside the batholith. However, as shown in Figure 12, the current apparent width of the formerly continuous batholithic rocks in West Antarctica near Thurston Island and Pine Island Bay is ~300 km (Kipf et al., 2012; Pankhurst et al., 1993), consistent with a widening of the batholith toward the east.

Our qualitative interpretation of the CMAS indicates that it is not necessarily reflecting prerift (pre-100 Ma) basement geology, but instead probably the occurrence of synrift (100–85 Ma) igneous rocks. The lateral extent of the anomalies implies that the area and volume of these rocks, which we herein term the Campbell Mafic Complex (CMC), is vast compared to the onland extent of magnetic portions of the Median Batholith. Magnetic susceptibility data from ~9,000 New Zealand igneous rocks (Table S7 and Figure S6) shows that most of these basaltic-gabbroic rocks have susceptibilities 1–2 orders of magnitude greater than that of most rhyolitic-granitic igneous rocks, supporting our suggestion that the magnetic source is more likely to be mafic, rather than felsic. Within Zealandia, there are several scattered occurrences of Late Cretaceous igneous rocks (Tulloch, Ramezani, Mortimer, et al., 2009; Timm et al., 2010, Mortimer, Gans, et al., 2017, and references therein). The only onshore rocks of South Zealandia that might be related to the CMAS are circa 85 Ma alkaline basalt-trachybasaltic Southern Volcanics of Pitt Island, The 97 Ma weakly A-type granites of the Auckland Islands and Takahe dredge site probably are also representative of this widespread magmatism within South Zealandia. Thus, they are representative of at least some of the rocks that comprise the CMC. Alkaline lamprophyre dyke swarms of North Zealandia are also highly magnetic and are associated with the Paparoa Metamorphic Core Complex on the Tasman Sea margin (Tulloch & Kimbrough, 1989; van der Meer et al., 2016). Associated magnetic anomalies do not extend to

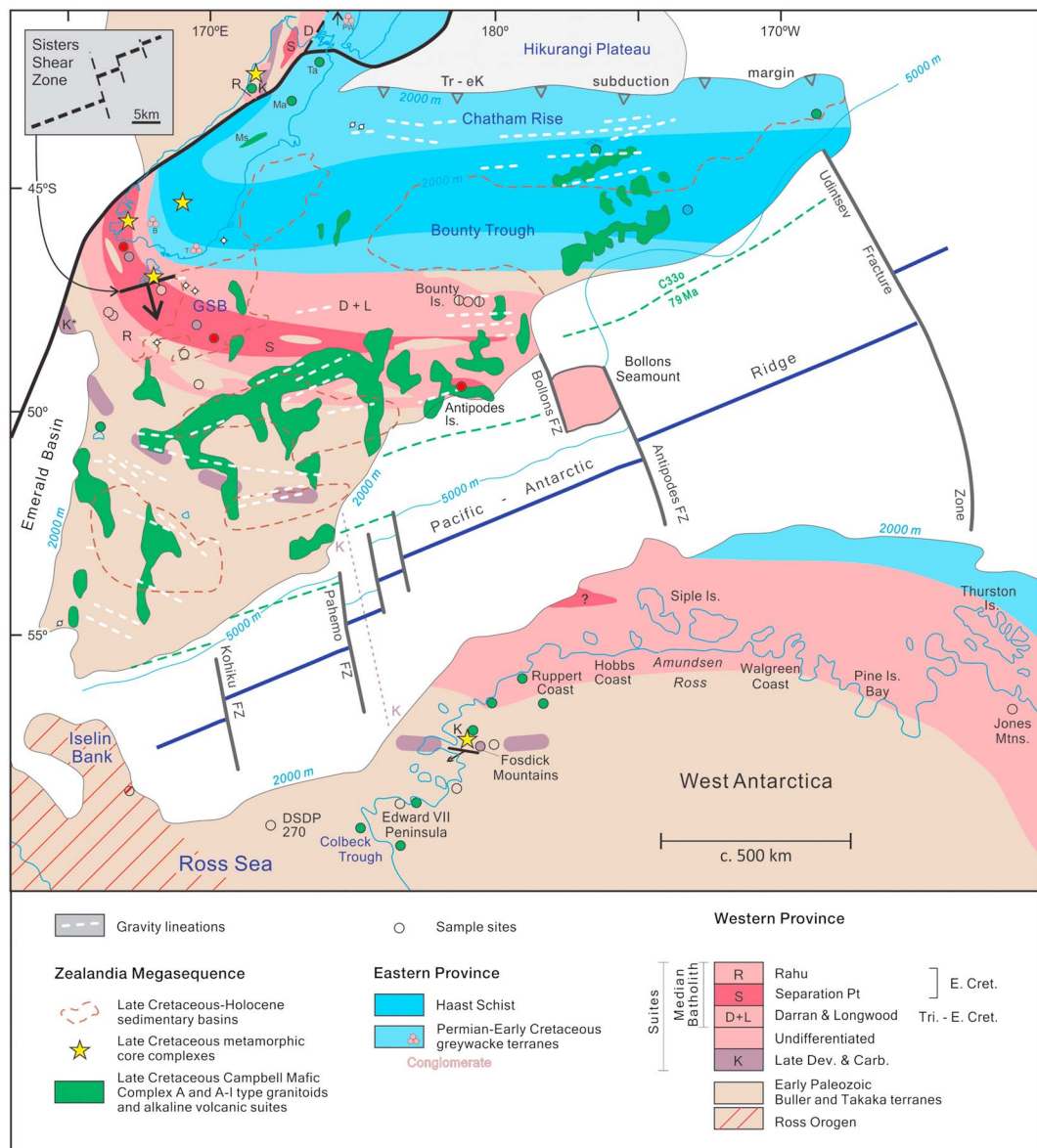


**Figure 12.** Geological map ~1:25 M scale showing offshore South Zealandia and the West Antarctic conjugate margin. At circa 74 Ma (modified after Sutherland, 1999). Onshore New Zealand geology is represented in its current configuration. The east-west orientation of Median Batholith from southern South Island is suggested by the orientation of the Chatham margin and accretionary wedge and confirmed by the character of basement at Bounty and Antipodes Islands. CMC is essentially represented by our outline of the Campbell Magnetic Anomaly System but excludes those magnetic anomalies that can be ascribed to JMA/SMAS and Median Batholith onshore and near shore, and offshore anomalies that can be linked to Late Cenozoic alkali volcanism (Pukaki Rise; Timm et al., 2010). Karamea Suite S-type granite is a major, latest Devonian, flare-up event that is also recognized in SE Australia and West Antarctic sectors of the SE Gondwana margin (Tulloch et al., 2017). Rahu Suite is widespread within and west of Karamea Batholith (K) in Westland. Sisters Shear Zone arrow is mean ductile lineation trend and transport direction of upper plate. Offsets on detachment fault are inferred from Kula et al. (2009). Ms = Mount Somers; Ma = Mandamus; Ta = Tapuae-o-Uenuku. West Antarctic data are from Siddoway et al. (2004; Colbeck Trough), Siddoway (2008; Fosdick detachment fault), Siddoway and Fanning (2009), and Yakymchuk et al. (2015; for late Devonian ages in the Fosdick Mountains). The Iselin Bank dredge sample is described in Mortimer et al. (2011).

the immediate offshore region; however, major magnetic anomalies beginning ~250 km further northwest that is subparallel to the Tasman margin are approximately colinear to these North Westland dyke swarms (e.g., Sutherland, 1999). Extrapolation of the CMAS anomaly to the southwest on a circa 100 Ma

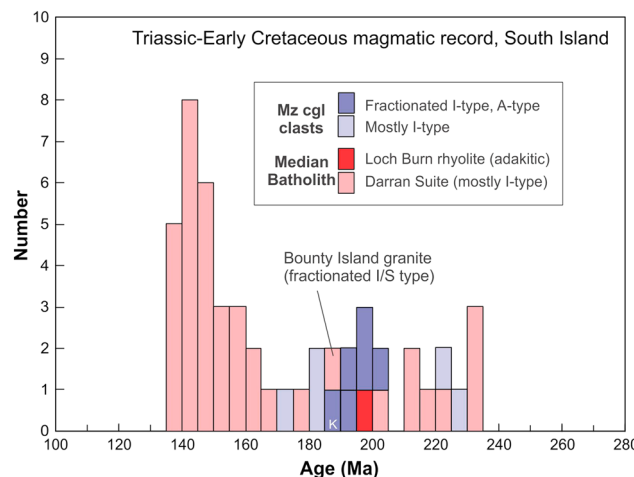


**Figure 13.** Ages of Bounty Island granite and clasts from Jurassic forearc basins appear to lie within a general lull in the onshore record of Darran Suite magmatism.

1999; Wandres et al., 2004; Keeman & Palin, 2013; Mortimer et al., 2015). This tentatively suggests that plutons of this age may be more widespread in the Median Batholith and its offshore continuation than previously recognized (as generally indicated by Nelson & Cottle, 2017).

### 4.3. Zealandia-West Antarctica Basement Comparisons

As noted by many authors including Grindley and Davey (1982) and Wobbe et al. (2012), the conjugate continental margins of Campbell Plateau and West Antarctica west of Thurston Island fit together well, especially west of the Antipodes Fracture Zone. In West Antarctica, Pankhurst et al. (1998) defined Ross and Amundsen geological provinces. The Amundsen Province, dominated by Permian-Mesozoic plutonic rocks, was regarded by Pankhurst et al. (1998) as a correlative of New Zealand's Median Tectonic Zone (now Median Batholith). The Ross Province, with its Early Paleozoic metasedimentary rocks, and Devonian plutonic rocks, was regarded by them as a correlative of New Zealand's Western Province terranes and Karamea Batholith.

The Antarctic continental margin cuts very obliquely across basement trends in West Antarctica, so the strike of the Amundsen-Ross province boundary is imprecisely defined. Nonetheless the spatial fit with projected E-W Zealandia basement trends is good and, we believe, provides a reliable falsification of NW-SE basement trends on the Campbell Plateau, for example, as interpreted by Sutherland (1999) and Frogtech (2013).

West Antarctic and Zealandian batholithic rocks match in time as well as space. A compilation of previously published age data on Mesozoic West Antarctica plutons shows a broadly similar trimodal age pattern to that of the Median Batholith (Figure 14), despite the variety of geochronological methods used. However, the post-130 Ma plutonic rocks in West Antarctica (from Thurston Island to the Ross Sea) do not have the strong adakitic (high Sr/Y) geochemical features of the Separation Point Suite in New Zealand (Figure 15). Further to the east in Palmer Land adakitic granites are present (e.g., Wareham et al., 1997). Here their relatively subdued Sr/Y values are better compared with those of the Peninsular Ranges batholith of Baja-California than the Median Batholith (Tulloch & Kimbrough, 2003), and both the PRB and Antarctic Peninsular batholiths show more consistent margin-parallel magnetic anomalies (Ferraccioli et al., 2006) than those associated with the Median Batholith.

Paleozoic continental margin arc rocks also appear to provide a second piercing point between South Zealandia and West Antarctica. Devonian-Carboniferous (375–340 Ma) granitoids within the Ross Province of West Antarctica have been broadly correlated with Paleozoic terranes and suites in New Zealand (Pankhurst et al., 1998), which themselves have been correlated with similar rocks in SE Australia (Cooper & Tulloch, 1992; Muir et al., 1996). This supports the overall fit of prebreakup geology between the now-separated continents. In particular, a belt of Karamea Suite high-flux magmatism at

reconstruction (e.g., Figure 1 inset) would intersect North Zealandia in South Westland where van der Meer et al. (2016) report circa 100 Ma calc-alkaline lamprophyres, some 400 km south on a Cretaceous reconstruction, of the highly magnetic North Westland dykes. No magnetic anomalies are associated with the calc-alkaline dykes.

### 4.2. Early Jurassic Granites of Zealandia

The 196- to 188-Ma ages reported here represent an age within the Darran Suite that is not well represented by in situ on-land plutons (Mortimer et al., 1999, 2015). Rocks with ages most similar are diorites of the Pahia Intrusives at Cosy Nook (samples CNP and BB30;  $203.2 \pm 2.8$  Ma and  $211.0 \pm 3.4$  Ma; Price et al., 2006), and a Loch Burn rhyolite (ca. 195 Ma, Kimbrough et al., 1994). Cosy Nook diorites are of typical Darran Suite character (Price et al., 2011). However, Loch Burn rhyolite has a weak adakitic character (Figure 8), somewhat different to both typical Darran Suite and Bounty Island granite compositions.

Despite the dearth of in situ Early Jurassic plutons, dated clasts of Early Jurassic (ca. 205–170 Ma) granitoids occur (Figure 13) in several Jurassic and Cretaceous Zealandian conglomerates (Figure 9; Tulloch et al.,

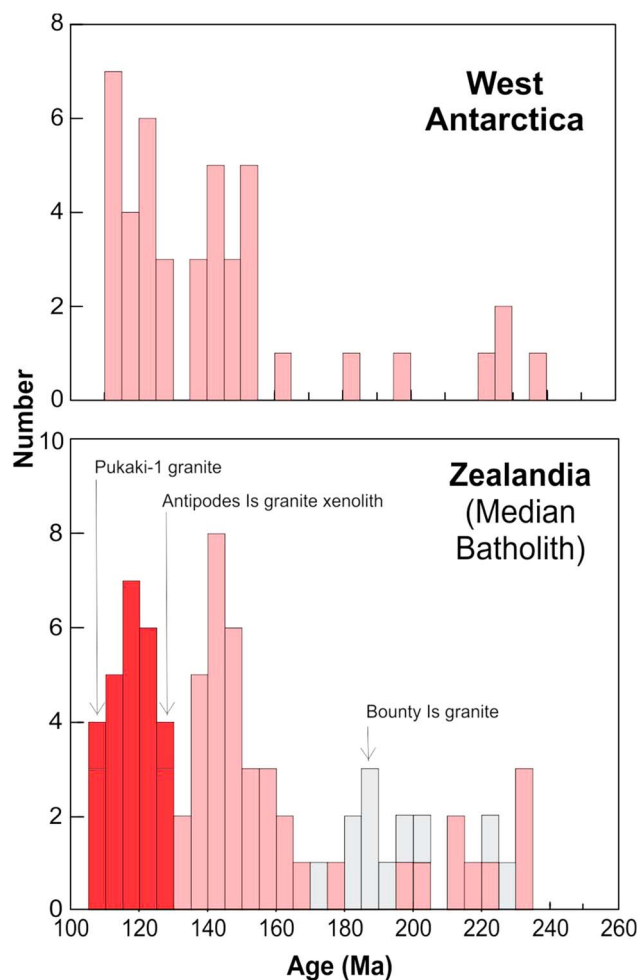


**Figure 14.** Histogram of Triassic-Early Cretaceous (240–100 Ma) magmatism in West Antarctica (Thurston Island to King Edward IV peninsular;  $n = 43$ , errors nominally  $\pm 5$  Ma) compared with the Median Batholith of New Zealand. Data sources: Pankhurst et al. (1993, 1998; Rb-Sr) and Mukasa and Dalziel (2000; multigrain TIMS U-Pb). Median Batholith ( $n = 65$ , errors all nominally  $\pm 3$  Ma) multigrain TIMS U-Pb, Tulloch and Kimbrough (2003) and Kimbrough et al. (1994); secondary ion mass spectrometry, Muir et al. (1994, 1998), Waight et al., 1997), and references in Mortimer et al. (2015). TIMS = thermal ionization mass spectrometry.

$370 \pm 1$  Ma, located inboard of the Median Batholith in New Zealand appears to be matched by a strong  $370 \pm 1$  Ma magmatic signal in granitic rocks of the Fosdick Mountains of western Marie Byrd Land (Siddoway & Fanning, 2009; Yakymchuk et al., 2015). Although no Karamea Suite plutons have thus far been sampled in offshore South Zealandia, a distinctive  $370 \pm 1$  Ma signal appears in detrital zircon patterns of Late Cretaceous sandstones in the Great South basin, confirming the nearby presence of Karamea Suite plutons (Tulloch, Ramezani, Kimbrough, et al., 2009).

Scattered within Ross Province of West Antarctica is a suite of 101–95 Ma weakly A-type granitoids called Byrd Coast Granite (Weaver et al., 1992). Like the bulk of the Devonian-Carboniferous granitoids, these mostly lie well west and south of the Mesozoic batholith, and granites on Auckland Island and The Snares are likely equivalents on South Zealandia. In a wider context, they probably are related to CMC magmatism.

#### 4.4. Multiphase Rifting, Failed Rifts, and Rheological Controls

Gravity lineations in Figure 3 strike in three separate directions. We suggest that two of these are associated with separate rift trends (Figure 16) that generally support the two-stage rifting model reported by Kula et al. (2007). The southern Campbell Plateau is dominated by gravity lineations that trend at  $\sim 130^\circ$ , a direction

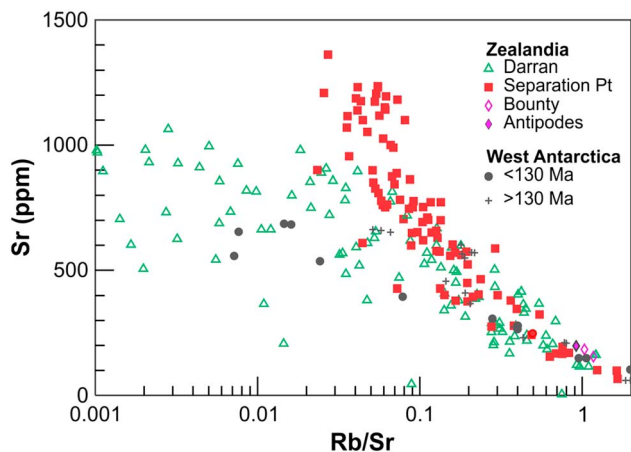


**Figure 15.** Comparison of Sr content of plutons in the Jurassic-Early Cretaceous Thurston Island-Pine Island Bay sector of the SE Gondwana margin arc. Data from Pankhurst et al. (1993) and Kipf et al. (2012). No rocks exhibit the high Sr content of the Separation Point Suite phase of the Median Batholith in the Zealandia.

that is broadly parallel to the axis of Colbeck Trough in formerly contiguous westernmost West Antarctica, the formation of which has been dated at circa 98 Ma (Luyendyk et al., 2003; Siddoway et al., 2004). This suggests the lineations may also be rift features and this is confirmed by the seismic section (Figure 10) across these lineations in the vicinity of Auckland Island. Because of these relationships we associate the ~130° trend with Ross Sea rifting of West and East Antarctica. This trend matches the early extension direction within the Great South basin (Sahoo et al., 2014), suggesting a circa 98 Ma age for the latter. A second set of gravity lineations are the ~090° trends on the Bounty Platform and Chatham Rise, near and parallel to the Bounty Trough that Eagles et al. (2004) suggested opened at circa 90 Ma. Grobys et al. (2007) suggested orthogonal opening via transitional pure to simple shear. We suggest that the asymmetry in seafloor and Moho depth (both deepest on the south side of the trough Grobys et al., 2007), might also be suggestive of lithospheric control via the contrast between strong Median Batholith to the south and weak accretionary wedge to the north (cf. Bot et al., 2016; Corti et al., 2018) effectively guiding the rifting along the north edge of the batholith. The oblique orientation of this path (Figure 11) is also mechanically favored (e.g., Heine & Brune, 2014). At the western end of the Bounty Trough, rifting, as suggested by Eagles et al. (2004), abruptly turns 80° to the south, possibly rebuffed by the southeastern edge of the subducted Hikurangi Plateau (Reyners et al., 2017), but appears to stall over the Median Batholith in the Great South basin. The 90 Ma age suggested by Eagles et al. (2004) corresponds to the inception of fast cooling during tectonic exhumation of the lower plate of the Sisters detachment. Thus, Bounty Trough rifting was conceivably formed by en echelon rifting (Eagles et al., 2004; Grobys et al., 2007) driven by the same extension direction as that of the Sisters Shear Zone, with which it eventually connected. The third set of gravity lineations trends ~070° across the central Campbell Plateau and most are coincident with the dominant section of the CMAS. As discussed above, alkaline magmatism and continental deformation associated with this trend is circa 89–80 Ma, some 10–12 Ma younger than the Colbeck-related lineations. As such we associate it with extension related to final West Antarctica-South Zealandia rupture (Stage 2 of Kula et al., 2007).

If these basins, gravity lineations and ductile features do indeed define datable orthogonal extension directions, then, tentatively, extension within South Zealandia stepped counterclockwise from circa 101–89 Ma to 90–80 Ma, supporting the two rift stages of Kula et al. (2007). Late Cretaceous counterclockwise rotation of extension with time has also been described in deep arc crust now exposed in Fiordland, and the Westland block of North Zealandia (Figure 16). The older event in Fiordland (Klepeis et al., 2016) is temporally and kinematically matched by the mid-Cretaceous (101–97 Ma, Raine et al., 2018) Puysegur Group basin. Slightly older (ca. 109 Ma) extension reported in eastern Fiordland by Scott and Cooper (2006) is oblique to the intraplate Klepeis et al. (2016) trends and apparently arc-parallel; we suggest this extension is more likely to be associated with arc processes.

In Westland the Paparoa Metamorphic Core Complex (Tulloch & Kimbrough, 1989; Tulloch & Palmer, 1990; Klepeis et al., 2007; Schulte et al., 2014) of North Zealandia (Figure 16) is represented by 101 Ma graben formation and rapid cooling during 102–89 Ma (half-graben tuff, Tulloch, Ramezani, Mortimer, et al., 2009; muscovite and K-feldspar Ar-Ar, Spell et al., 2000) associated with the Ohika detachment fault. The age of the southern detachment (Pike) is less well constrained, but an age for hydrothermal muscovite on the detachment of circa 84 Ma contrasts with 98 Ma for similar on the Ohika detachment (Spell et al., 2000; Tulloch & Palmer, 1990) is also apparent. These two events are matched by two episodes of calc-alkaline and alkaline lamprophyric magmatism in North Zealandia reported by Adams and Nathan (1978) and van der Meer et al. (2016).

Some authors have suggested intraplate extension initiated significantly earlier, at circa 110–116 Ma. While we do not discount the possibility that extension began earlier than circa 102 Ma we suggest that current evidence for this is not compelling. Tulloch and Kimbrough (1989) based a 110 Ma age on a biostratigraphic assignment for the Stitts tuff that was circa 10 Ma too old (Muir et al. 1997; Tulloch, Ramezani, Mortimer,

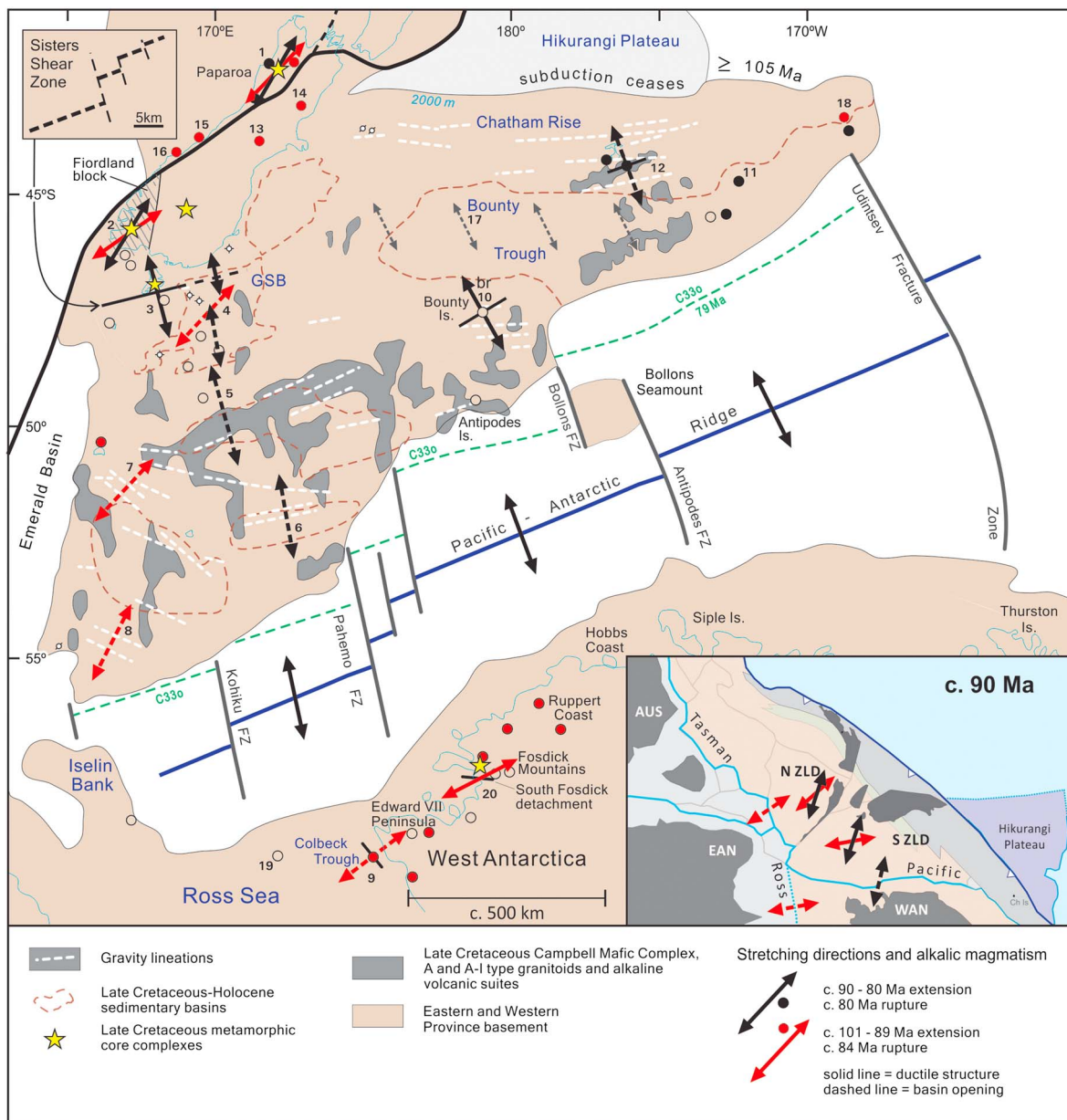


**Figure 16.** Kinematic map of South Zealandia and nearby blocks of North Zealandia (Westland) showing extension directions for circa 95 and circa 85 Ma rifting events. Counterclockwise rotation of extension direction from old to young events is indicated. Such rotation is also apparent in the Fiordland block and in the Paparoa core complex of North Zealandia. Note that North Zealandia (and to a lesser extent the Fiordland block) should be rotated counterclockwise for strict comparison of regional extension orientations. See Figure 1 inset for approximate reconstruction that includes summary extension directions for North and South Zealandia. Apparent rotation of extension direction from early to late is largely due to variation in orientation of stage 1 extension. Bounty Trough is undated but is apparently older than the third inferred circa 85 Ma Campbell Magnetic Anomaly System belt south of Chatham Islands and may be circa 90 Ma. Small arrows denote suggested oblique extension in Bounty Trough as discussed in the text. Age ranges are stage 1, 101–89 Ma; stage 2, 90–80 Ma, with the lower ages of each stage determined by  $^{40}\text{Ar}$ - $^{39}\text{Ar}$  thermochronology of K-feldspar (Kula et al., 2009; Spell et al., 2000). Extension directions given for basins are assumed orthogonal unless otherwise noted. Inset shows a regional context for stage 1 (Ross-Tasman, red), and stage 2 (Pacific, black) basin opening events. Rupture ages are circa 84 Ma (a little before Chron 34y) for Tasman margin and circa 80 Ma (a little before Chron 330) Pacific margin (Cande & Stock, 2004). Numbered locations are references to kinematics/igneous character/age: 1 = Paparoa Metamorphic Core Complex (Klepeis et al., 2007; Schulte et al., 2014; Tulloch & Kimbrough, 1989; van der Meer et al., 2016); circa 84 Ma alkaline magmatism (Adams & Nathan, 1978; van der Meer et al., 2018); 2 = Fiordland (Klepeis et al., 2016); 3 = Sisters Shear Zone of Pegasus metamorphic core complex (Kula et al., 2009; Ring et al., 2015); 4 = Great South basin, early extension (Sahoo et al., 2014), late extension: NW margin of basin (Frogtech, 2013), Pakaha Horst Cook et al., 1999); 5, 6 = Pukaki basins (Frogtech, 2013); 7 = New basin, Figure 11c herein; 8 = Similar gravity anomalies to 7; 9 = Siddoway et al. (2004); 10 = Bounty Island brittle faults described herein; 11 = three dredged basaltic and trachytic intraplate rocks (Mortimer et al., 2019); 12 = Pitt Island alkali basalt (Panter et al., 2006) and trachyandesite (herein); 13 = Mount Somers rhyolite (van der Meer et al., 2017); 14 = Mandamus Complex (Tulloch, 1991); 15 = Rhyolite (Phillips et al., 2005); 17 = Bounty Trough, possible oblique rifting as discussed in text; 18 = Takahe dredge sample (Mortimer et al., 2006); 19 = Deep Sea Drilling Project well 270 (Fitzgerald & Baldwin, 1997); 20 = Fosdick Mountains (McFadden et al., 2015).

et al., 2009). Waight et al. (1998) concluded that the mylonitic deformation of 110 Ma Buckland Pluton at the northern end of the Paparoa Metamorphic Core Complex could have been syntectonic, noting a temporal association with an apparent regional magmatic pulse at this time, but no evidence for or against a *post* magmatic origin was presented. However, Spell et al. (2000) noted that the bulk of extension in the Paparoa core complex was on the southern, Pike detachment fault, more distant from such plutons. Although Spell et al. (2000) also indicated that extension may have initiated by 110 Ma, they report rapid cooling began during muscovite closure at circa 102 Ma (overlapping Stitts tuff), whereas the older hornblende ages overlap zircon crystallization age, suggesting to us that this early cooling was isobaric. Sagar and Palin (2011) reported a  $105 \pm 2$  Ma age for a syntectonic dyke in the Paparoa core complex. However, we now consider the age on this complex zircon pattern to be slightly younger, possibly overlapping with the Stitts Tuff in the associated half graben. Schulte et al. (2014) reported a Rb/Sr isochron age of  $116 \pm 6$  Ma from a granitic ultramylonite also on the southern end of the Paparoa core complex. However, the high MSWD and likely Paleozoic S-type granite protolith indicate that an older age due to a small amount of incomplete resetting cannot be excluded. Alternatively, the Rb/Sr age might reflect the 116- to 117-Ma thermal pulse associated with the largest phase of Median batholith construction (Schwartz et al., 2017). Extension may have been underway in the lowermost crust in Fiordland by circa 105 Ma (Klepeis et al., 2016). Support for a circa 100- versus 110-Ma initiation of extension also comes from biostratigraphy—the bases of eight out of 10 nonmarine synrift basins across New Zealand line up at a maximum age of 99–101 Ma. The only older basin (Kyeburn; Tulloch, Ramezani, Mortimer, et al., 2009) is likely arc related.

These two cooling/extension events across both South and North Zealandia (101–89 Ma and 90–80 Ma) are also recognized in western Marie Byrd Land (Fitzgerald & Baldwin, 1997; Lisker & Olesch, 1998; Richard et al., 1994; Siddoway et al., 2004). Rapid cooling in the Fosdick Mountains (McFadden et al., 2015) from circa 100–95 Ma is associated with exhumation on the South Fosdick detachment fault with ductile stretching lineations subparallel to inferred Colbeck Trough extension and stage 1 extension in South Zealandia. The clear pattern established here for Antarctica-NZ rifting confirms our previous assertion (Tulloch, Ramezani, Mortimer, et al., 2009) that there is no evidence in the kinematics for plume-driven rifting (Storey et al., 1999). On a wider Zealandia scale (Figure 16 insert) stage 1 is associated with rifting of Zealandia and West Antarctica from Australia and East Antarctica (Ross-Tasman event), and stage 2 is associated with rifting of Zealandia from West Antarctica (Pacific event). Despite stage 1 extension beginning at least 11 Ma before stage 2, continental rupture associated with stage 2 followed stage 1 rupture by <5 Ma. In the large Taranaki Basin of North Zealandia Strogen et al. (2017) report 2 broad phases of rifting; our two stages essentially correspond to their early, “Zealandia rift” phase.

Broadly, we interpret the CMC as igneous rocks associated with a failed rift that preceded Gondwana supercontinent breakup, and subsequently formed South Zealandia and West Antarctica. One plausible reason for failure along the main CMC trend, with final breakup mostly east of the CMC, might be have been the stronger, thicker, garnet-rich Separation Point Suite Median Batholith arc root recognized in the lower crust now exposed in Fiordland (Klepeis et al., 2016) in the South Zealandia sector of the batholith. Adakitic granites associated with this strong deep root are apparently absent in contiguous West Antarctica west of Palmer Land. Rifting may thus have been partitioned eastward toward weaker, nonadakitic, arc segments. Such an effect might also be seen in the more fragmented nature of the CMC where it intersects and attempts to cut the likely path of the Median Batholith in the vicinity of the Bounty Platform.

How did such a large area of continental crust become thinned to an average of ~18–20 km (Groby et al., 2008) without rupturing into oceanic crust? We speculate that this extensive lateral thinning was achieved before eventual breakup because the crust was stretched in two distinctly different extension directions over 20 Ma.

#### 4.5. Magma-Rich or Magma-Poor Margin?

Passive rifted margins are commonly described in terms of two end-members, magma-rich and magma-poor (e.g., Doré & Lundin, 2015; Franke, 2013). Magma-poor margins are hyperextended, exhume mantle, and are apparently restricted to margins where breakup of the crust break up preceeds breakup of the lithospheric mantle. At magma-rich margins, the lithospheric mantle breaks before or during crust breakup and produces large volumes of synrift volcanic rocks recognized as seaward dipping reflectors.

The 2,450-km-long Campbell-Chatham margin of South Zealandia can be divided into three sectors, based on bathymetry and apparent COB zone width. The southern sector as far north as the intersection with the Pahemo Fracture Zone (latitude  $\sim 53^{\circ}20'$ ) apparently has a relatively narrow COB:  $\sim 70$  and 130 km from 2- to 5-km water depth. To the north of the Pahemo Fracture Zone the width of the COB everywhere ranges from  $\sim 230$  to 270 km. The margin in the northernmost sector is hyperextended to the extent that continental rocks extend to  $\sim 5,000$  m below sea level (Mortimer et al., 2019). Fast early sea-floor half-spreading rates (calculated from seafloor spreading anomalies C33o-C32 in Sutherland, 1999) of  $\sim 3$  cm/year in the north and 1.5–2 cm/year in the southern sector more consistent with volcanic-rich margins (all sectors record much faster spreading than mostly coeval spreading in the Tasman Sea). However, absence of seismic lines across the Campbell margin means the presence of seaward dipping volcanic reflectors cannot be assessed. While the apparent fast spreading rate and apparent narrow necking zone might be consistent with the possibility of such in the southern sector, hyperextension in the northern, Chatham Rise-Bounty Trough, sector is probably inconsistent with a volcanic margin. On the West Antarctic conjugate margin Wobbe et al. (2012) report a broadly similar E-W variation along that margin, with the eastern segment hyperextended. Although they found no seaward dipping seismic reflectors characteristic of synrift volcanism that appears anomalous given reported the rapid extension rates during initial seafloor spreading that typically is associated with volcanic margins (Doré & Lundin, 2015).

Magnetic anomalies in the Amundsen Sea Embayment reported by Gohl et al. (2013) share some similarities to the CMAS, although contributions from continental margin arc rocks, or even younger rifting, cannot be discounted, especially as Ferraccioli et al. (2006) map a major subduction margin-parallel magnetic anomaly to the outboard belt of the Antarctic Peninsular Batholith to the east along the margin in Palmer Land. Gohl et al. (2013) also note that some of the northern magnetic anomalies in the Amundsen Sea are suggestive of seaward dipping reflectors of volcanic-rifted margins (e.g., Doré & Lundin, 2015; Franke, 2013). However, as discussed above, the conjugate margin SE of the Chatham Islands is not likely to be volcanic.

#### 4.6. Cryptic, Yet Dominant, Rift-Related Geology

As outlined above, we interpret that Late Cretaceous igneous rocks and structures likely underlie much of the Campbell Plateau. The main evidence for this is the parallelism of the orthogonal elements of the CMAS to structures related to synrift extension (Sisters Metamorphic Core Complex) and postrift extension (Southern Ocean transform faults and spreading segments). The recognition that the Campbell Plateau may be dominated by a cryptic rift-related geological unit supports earlier interpretations of widespread extension in South Zealandia. As well as the obvious deep sedimentary basins and Sisters Metamorphic Core Complex (Cook et al., 1999; Kula et al., 2007), Eagles et al. (2004) and Grobys et al. (2007) suggested that early rifting formed the Bounty Trough before stalling in the Great South basin. Grobys et al. (2008) reported gravity data that they interpreted as *en echelon* extensional features associated with nascent sea floor spreading in the Bounty Trough. East-west gravity lineations on the Bounty Platform may be related to this event, whereas pervasive brittle structures (Figure S1) in Bounty Islands granite trend  $\sim 060^{\circ}$  (the average of predominant structure or rock elongation direction from 11 islets). This fabric is thus subparallel to the youngest rift structures, the Sisters Shear Zone/CMAS/MOR, and overprints the Bounty Trough trend (as does the CMAS). The Late Cretaceous Tupuangi Formation in the Chatham Islands was deposited in a NNE-trending extensional half graben (Campbell et al., 1993; Wood & Anderson, 1989) that is exposed in northern Pitt Island. The youngest population of detrital zircons from a Tupuangi Formation sandstone has a mode circa 97 Ma (Adams, 2008). The 97 Ma zircon provides a maximum stratigraphic age and were derived from rare intraplate magmatism that was widespread over Zealandia (Tulloch, Ramezani, Mortimer, et al., 2009), including the easternmost Chatham Rise. These features are entirely consistent with continental scale extension that led to the observed 12–24 km thickness (Grobys et al., 2008) of South Zealandia.

#### 4.7. Constraints on Age and Origin of the New Zealand Orocline

A wide range of ages (Early Cretaceous to Miocene-Recent) have been postulated for the north and south bends of the Z-shaped oroclinal deflection in New Zealand basement terranes. A recent review by Mortimer (2014) summarized that the age of the bend in the North Island was pre-Eocene (Bradshaw et al., 1996), in the Marlborough part of South Island was Neogene and in the Fiordland part of South Island was problematic. Subsequently, Lamb et al. (2016) suggested the Fiordland part of the oroclinal bend was probably pre-Eocene. In Figure 12 we show that the Late Cretaceous Sisters Shear Zone is parallel to

long baseline features outside the orocline—the CMAS and the latest Cretaceous Pacific spreading ridge. In other words, it has not been rotated by the orocinal bend. Thus, at least 50° of rotation of the Fiordland orocinal bend predates (youngest) 93–82 Ma (Kula et al., 2009) continental extension and rupture. Given that the youngest bent plutonic rocks in this sector of the batholith were emplaced at circa 105 Ma (Allibone & Tulloch, 2008; Tulloch & Kimbrough, 2003), the bending of these basement rocks between Stewart Island and Fiordland is constrained (cf Lamb et al., 2016) to within 105–93 Ma. This timing supports the suggestion of Reyners et al. (2017) that collision of the Hikurangi Plateau with the Gondwana margin during this interval caused this major vertical axis rotation.

#### 4.8. Further Work

We acknowledge that our treatment of magnetic and gravity anomalies in this paper is qualitative, not quantitative. We hope that our speculative interpretations and the new regional geological context will drive new geophysical investigations. Formal modeling of potential field data across the Campbell Plateau would be a sensible next step in the interpretation of the geology, for example, to determine igneous rock characteristics, volumes, and depths and to directly compare gravity and seismic sections.

### 5. Conclusions

Based on a small number of samples from island outcrops, volcanic xenoliths and oil exploration wells, Carboniferous to Early Cretaceous plutonic rocks can be traced across the Campbell Plateau of South Zealandia. We interpret the Median Batholith of onshore New Zealand to continue with west-east strike, from Stewart Island to the Bounty Platform. Prior to Gondwana breakup, the Median Batholith of South Zealandia was colinear with the Amundsen Province of West Antarctica (Pankhurst et al., 1998). Despite a good match in Permian to Cretaceous igneous pulses and lulls in the batholithic rocks of Zealandia and West Antarctica, adakitic suites appear restricted to Zealandia. The inferred east-west strike of the Median Batholith across the Campbell Plateau is parallel to the inferred east-west strike of the Haast Schist from the South Island coast to the Chatham Islands.

#### Acknowledgments

We thank Hamish Campbell, Moses Turnbull, James Scott, New Zealand Oceanographic Institute (now NIWA), and Randall McDonnell for help in obtaining samples. Technical and analytical assistance was provided by Nick Walker (TIMS geochronology), Dave Parkinson (radiogenic isotopes), John Simes (rock crushing and mineral separations), Belinda Smith Lyttle (mineral separations and graphics), Steve Tulloch (photomacographs), and Jenny Black (magnetic data sets). We thank Fred Davey, Karsten Gohl, Bryan Davy, Christine Siddoway, and Donna Eberhart-Phillips for discussion and comments. Keith Klepeis provided a reconnaissance structural analysis of Bounty Island and discussion of Paparoa core complex development. Journal reviewers Quinten van der Meer and Fausto Ferraccioli are thanked for comments that significantly improved the manuscript. Christine Siddoway generously provided analyses of granite samples from the Colbeck Trough. The work was supported by Core Research Funding to GNS Science by the New Zealand Government Ministry of Business, Employment and Innovation. More context for data reported here may be found in the Petlab database: <https://pet.gns.cri.nz/pet/>.

The CMAS has an orthogonal pattern that is parallel and perpendicular to demonstrable extension-related structures at its margins. We propose that the CMAS relates to a large Late Cretaceous, rift-related, mainly mafic, igneous complex (CMC), rather than basement terranes or batholiths, thus removing the original argument for a strike-slip “Campbell Fault.”

Extensional deformation of South Zealandia rotated counterclockwise between two main stages spanning a total of circa 20 Ma. Stage 1 extension (ca. 101–89 Ma) between proto-Zealandia/West Antarctica and East Antarctica/Australia led to rupture and first Tasman Seafloor at slightly before 83 Ma (Chron34). Stage 2 extension (ca. 90–80 Ma) between Zealandia and West Antarctica led to rupture and first Pacific seafloor after 83 Ma, but before 79 Ma (Chron33o). Alkaline magmatism in North Zealandia matches these two stages of extension. Variation in extension direction may have allowed the 1.5-Mkm<sup>2</sup> region of South Zealandia to be stretched without rupturing to form new ocean crust. Because the Sisters Shear Zone cuts a 105 Ma pluton in the south limb of the New Zealand orocline at least 50° of rotation of the south limb is apparently constrained to within 105–93 Ma, supporting the suggestion that bending was caused by collision of the Hikurangi Plateau with the subduction margin.

The geology and exhumation history of the igneous and metamorphic rocks of the Campbell Plateau and Chatham Rise are thus now well characterized in terms of the few available samples (this study; Mortimer et al., 2016). Now that these basics are established, an assessment of the changing kinematic direction of Zealandia and West Antarctica extension during the 100- to 85-Ma synrift period can follow.

### References

- Adams, C. (2008). Geochronology of Paleozoic terranes at the Pacific Ocean margin of Zealandia. *Gondwana Research*, 13, 250–258.
- Adams, C., Mortimer, N., Campbell, H., & Griffin, W. (2015). Detrital zircon ages in Buller and Takaka terranes, New Zealand: Constraints on early Zealandia history. *New Zealand Journal of Geology and Geophysics*, 58(2), 176–201. <https://doi.org/10.1080/00288306.2015.1025798>
- Adams, C. J. (1983). Age of the volcanoes and granite basement of the Auckland Islands, Southwest Pacific. *New Zealand Journal of Geology and Geophysics*, 26(3), 227–237. <https://doi.org/10.1080/00288306.1983.10422237>

- Adams, C. J. (1985). Geology of the Antipodes and Bounty Islands, southwest Pacific: Report of geological studies on the 1985 subantarctic cruise of HMNZS Monowai northern leg to Antipodes and Bounty Islands 27 February–13 March 1985. Lower Hutt: DSIR, Institute of Nuclear Sciences. Institute of Nuclear Sciences Report INS-R-300.25 p.
- Adams, C. J., Campbell, H. J., & Griffin, W. (2008). Age and provenance of basement rocks of the Chatham Islands: An outpost of Zealandia. *New Zealand Journal of Geology and Geophysics*, 51(3), 245–259. <https://doi.org/10.1080/0028830089509863>
- Adams, C. J., Campbell, H. J., Mortimer, N., & Griffin, W. L. (2017). Perspectives on Cretaceous Gondwana break-up from detrital zircon provenance of southern Zealandia sandstones. *Geological Magazine*, 154, 661–682.
- Adams, C. J., & Cullen, D. J. (1978). Potassium-argon ages of granites and metasediments from the Bounty Islands area, southwest Pacific Ocean. *Journal of the Royal Society of New Zealand*, 8, 127–132.
- Adams, C. J., & Nathan, S. (1978). Cretaceous chronology of the lower Buller Valley, South Island, New Zealand. *New Zealand Journal of Geology and Geophysics*, 21(4), 455–462. <https://doi.org/10.1080/00288306.1978.10424070>
- Adams, C. J., Pankhurst, R. J., Maas, R., & Millar, I. L. (2005). Nd and Sr isotopic signatures of metasedimentary rocks around the South Pacific margin and implications for their provenance. In A. P. M. Vaughan, P. T. Leat, & R. J. Pankhurst (Eds.), *Terrane processes at the margins of Gondwana* (pp. 113–141). London: Geological Society (London) Special Publication 246.
- Adams, C. J., & Robinson, P. (1977). Potassium-argon ages of schists from Chatham Island, New Zealand Plateau, southwest Pacific. *New Zealand Journal of Geology and Geophysics*, 20(2), 287–301. <https://doi.org/10.1080/00288306.1977.10420708>
- Allibone, A. H., Jongens, R., Turnbull, I. M., Milan, L. A., Daczko, N. R., De Paoli, M. C., & Tulloch, A. J. (2009). Plutonic rocks of western Fiordland, New Zealand: Field relations, geochemistry, correlation, and nomenclature. *New Zealand Journal of Geology and Geophysics*, 52(4), 379–415. <https://doi.org/10.1080/00288306.2009.9518465>
- Allibone, A. H., & Tulloch, A. J. (2004). Geology of the plutonic basement rocks of Stewart Island, New Zealand. *New Zealand Journal of Geology and Geophysics*, 47(2), 233–256. <https://doi.org/10.1080/00288306.2004.9515051>
- Allibone, A. H., & Tulloch, A. J. (2008). Early Cretaceous dextral transpressional deformation within the Median Batholith, Stewart Island, New Zealand. *New Zealand Journal of Geology and Geophysics*, 51(2), 115–134. <https://doi.org/10.1080/00288300809509854>
- Allibone, A. H., Turnbull, I. M., Tulloch, A. J., & Cooper, A. F. (2007). Plutonic rocks of southwest Fiordland, New Zealand: Field relations, geochemistry and correlation. *New Zealand Journal of Geology and Geophysics*, 50, 283–314.
- Bache, F., Mortimer, N., Sutherland, R., Collot, J., Rouillard, P., Stagpoole, V., & Nicol, A. (2014). Seismic stratigraphic record of transition from Mesozoic subduction to continental breakup in the Zealandia sector of eastern Gondwana. *Gondwana Research*, 26(3–4), 1060–1078. <https://doi.org/10.1016/j.gr.2013.08.012>
- Beggs, J. M. (1978). Geology of the metamorphic basement and Late Cretaceous to Oligocene sedimentary sequence of Campbell Island, Southwest Pacific Ocean. *Journal of the Royal Society of New Zealand*, 8, 161–177.
- Beggs, J. M., Challis, G. A., & Cook, R. A. (1990). Basement geology of the Campbell Plateau: Implications for the Campbell Magnetic Anomaly System. *New Zealand Journal of Geology and Geophysics*, 33(3), 401–404. <https://doi.org/10.1080/00288306.1990.10425696>
- Black, L. P., Kamo, S. L., Williams, I. S., Mundil, R., Davis, D. W., Korsch, R. J., & Foudoulis, C. (2003). The application of SHRIMP to Phanerozoic geochronology: a critical appraisal of four zircon standards. *Chemical Geology*, 200(1–2), 171–188. [https://doi.org/10.1016/S0009-2541\(03\)00166-9](https://doi.org/10.1016/S0009-2541(03)00166-9)
- Bot, A., Geoffroy, L., Authemayou, C., Bellon, H., Grindorge, D., & Pik, R. (2016). Miocene detachment faulting predating EPR propagation: Southern Baja California. *Tectonics*, 35, 1153–1176. <https://doi.org/10.1002/2015TC004030>
- Bouvier, A., Vervoort, J., & Patchett, J. P. (2008). The Lu-Hf and Sm-Nd isotopic composition of CHUR: Constraints from unequilibrated chondrites and implications for the bulk composition of terrestrial planets. *Earth and Planetary Science Letters*, 272, 48–57.
- Bradshaw, J., Weaver, S., & Muir, R. (1996). Mid-Cretaceous oroclinal bending of New Zealand terranes. *New Zealand Journal of Geology and Geophysics*, 39, 461–468.
- Campbell, H. J., Andrews, P. B., Beu, A. C., et al. (1993). Cretaceous-Cenozoic geology and biostratigraphy of the Chatham Islands. *New Zealand Institute of Geological and Nuclear Sciences Monograph 2*, 1–94.
- Cande, S. C., & Stock, J. M. (2004). In N. Exon (Ed.), *Cenozoic reconstructions of the Australia-New Zealand-South Pacific sector of Antarctica*. Washington, DC: American Geophysical Union. <https://doi.org/10.1029/151GM02>
- Challis, G. A., Gabites, J., & Davey, F. J. (1982). Precambrian granite and manganese nodules dredged from the Campbell Plateau, New Zealand. *New Zealand Journal of Geology and Geophysics*, 25(4), 493–497. <https://doi.org/10.1080/00288306.1982.10421513>
- Chaput, J., Aster, R. C., Huerta, A., Sun, X., Lloyd, A., Wiens, D., et al. (2014). The crustal thickness of West Antarctica. *Journal of Geophysical Research: Solid Earth*, 119, 378–395. <https://doi.org/10.1002/2013JB010642>
- Cook, R. A., Sutherland, R., & Zhu, H. (1999). *Cretaceous-Cenozoic geology and petroleum systems of the Great South basin, New Zealand*. Institute of Geological and Nuclear Sciences Monograph 20 (p. 188). Lower Hutt: Institute of Geological and Nuclear Sciences.
- Cooper, R. A. (1989). Early Paleozoic terranes of New Zealand. *Journal of the Royal Society of New Zealand*, 19, 73–112.
- Cooper, R. A., & Tulloch, A. J. (1992). Early Paleozoic terranes in New Zealand and their relationship to the Lachlan Fold Belt. *Tectonophysics*, 214, 129–144.
- Corti, G., Molin, P., Sembroni, A., Bastow, I. D., & Keir, D. (2018). Control of pre-rift lithospheric structure on the architecture and evolution of continental rifts: Insights from the Main Ethiopian rift, East Africa. *Tectonics*, 37, 477–496. <https://doi.org/10.1002/2017TC004799>
- Cullen, D. J. (1965). Autochthonous rocks from the Chatham rise, east of New Zealand. *New Zealand Journal of Geology and Geophysics*, 8(3), 465–474. <https://doi.org/10.1080/00288306.1965.10426417>
- Cullen, D. J. (1975). Autochthonous rocks of the Bounty Islands region, south-west Pacific Ocean. *New Zealand Journal of Geology and Geophysics*, 18, 767–785.
- Dahlquist, J. A., Alasino, P. H., Eby, G. N., Galindo, C., & Casquet, C. (2010). Fault controlled Carboniferous A-type magmatism in the proto-Andean foreland (Sierras Pampeanas, Argentina): Geochemical constraints and petrogenesis. *Lithos*, 115(1–4), 65–81. <https://doi.org/10.1016/j.lithos.2009.11.006>
- Davey, F., & Christoffel, D. (1978). Magnetic anomalies across Campbell Plateau, New Zealand. *Earth and Planetary Science Letters*, 41, 14–20.
- Davidson, J., Turner, S., Handley, H., Macpherson, C., & Dosseto, A. (2007). Amphibole “sponge” in arc crust? *Geology*, 35(9), 787–790. <https://doi.org/10.1130/G23637A.1>
- Davy, B. (1993). The Bounty Trough—Basement structure influences on sedimentary basin evolution. In P. F. Ballance (Ed.), *South Pacific sedimentary basins* (pp. 69–92). Amsterdam: Elsevier science publishers. Sedimentary basins of the world 2.
- Davy, B. (2014). Rotation and offset of the Gondwana convergent margin in the New Zealand region following Cretaceous jamming of Hikurangi Plateau large igneous province subduction. *Tectonics*, 33, 1577–1595. <https://doi.org/10.1002/2014TC003629>

- Davy, B., Hoernle, K., & Werner, R. (2008). Hikurangi plateau: Crustal structure, rifted formation, and Gondwana subduction history. *Geochemistry, Geophysics, Geosystems*, 9, Q07004. <https://doi.org/10.1029/2007GC001855>
- De Paoli, M. C., Clarke, G. L., Klepeis, K. A., Allibone, A. H., & Turnbull, I. M. (2009). The eclogite-granulite transition: Mafic and intermediate assemblages at Breaksea Sound, New Zealand. *Journal of Petrology*, 50(12), 2307–2343. <https://doi.org/10.1093/petrology/egp078>
- Denison, R. E., & Coombs, D. S. (1977). Radiometric ages for some rocks from Snares and Auckland Islands, Campbell Plateau. *Earth and Planetary Science Letters*, 34, 23–29.
- Doré, T., & Lundin, E. (2015). Hyperextended continental margins—Knowns and unknowns. *Geology*, 43(1), 95–96. <https://doi.org/10.1130/focus012015.1>
- Eagles, G., Gohl, K., & Larner, R. D. (2004). High-resolution animated tectonic reconstruction of the South Pacific and West Antarctic Margin. *Geochemistry, Geophysics, Geosystems*, 5, Q07002. <https://doi.org/10.1029/2003GC000657>
- Ferraccioli, F., Jones, P., Vaughan, A., & Leat, P. (2006). New aerogeophysical view of the Antarctic Peninsula: More pieces, less puzzle. *Geophysical Research Letters*, 33, L05310. <https://doi.org/10.1029/2005GL024636>
- Field, B. D., & Browne, G. H. (1989). *Cretaceous and Cenozoic sedimentary basins and geological evolution of the Canterbury region, South Island, New Zealand*. DSIR, Wellington: New Zealand Geological Survey Basin Studies 2.
- Fitzgerald, P., & Baldwin, S. (1997). Detachment fault model for the evolution of the Ross embayment. In *The Antarctic region: Geological evolution and processes* (pp. 555–564). Siena: Terra Antarctica Publication.
- Fleming, C. A., Reed, J. J., & Harris, W. F. (1953). The geology of the Snares Islands. In *Cape expedition series, bulletin no 13* (pp. 9–31). Wellington, NZ: Department of Scientific and Industrial Research.
- Foley, F. V., Pearson, N. J., Rushmer, T., Turner, S., & Adam, J. (2013). Magmatic evolution and magma mixing of Quaternary adakites at Solander and Little Solander Islands, New Zealand. *Journal of Petrology*, 54(4), 703–744. <https://doi.org/10.1093/petrology/egs082>
- Franke, D. (2013). Rifting, lithosphere breakup and volcanism: Comparison of magma-poor and volcanic rifted margins. *Marine and Petroleum Geology*, 43, 63–87. <https://doi.org/10.1016/j.marpetgeo.2012.11.003>
- Frogtech (2013). *New Zealand extended continental shelf SEEBASE™. New Zealand petroleum and minerals report PR5063*. Wellington: Ministry of Business, Innovation and Employment.
- Frost, B. R., Barnes, C. G., Collins, W. J., Arculus, R. J., Ellis, D. J., & Frost, C. D. (2001). A geochemical classification for granitic rocks. *Journal of Petrology*, 42(11), 2033–2048. <https://doi.org/10.1093/petrology/42.11.2033>
- Gamble, J., & Adams, C. (1990). Antipodes Island. Volcanoes of the Antarctic Plate and Southern Oceans Antarctic Research Series. *American Geophysical Union*, 48, 468–469.
- Getty, S. R., & Gromet, L. P. (1992). Geochronological constraints on ductile deformation, crustal extension, and doming about a basement-cover boundary, New England Appalachians. *American Journal of Science*, 292(6), 359–397. <https://doi.org/10.2475/ajs.292.6.359>
- Gibson, G. M., McDougall, I., & Ireland, T. R. (1988). Age constraints on metamorphism and the development of a metamorphic core complex in Fiordland, southern New Zealand. *Geology*, 16(5), 405–408. [https://doi.org/10.1130/0091-7613\(1988\)016<0405:ACOMAT>2.3.CO;2](https://doi.org/10.1130/0091-7613(1988)016<0405:ACOMAT>2.3.CO;2)
- Gohl, K., Denk, A., Eagles, G., & Wobbe, F. (2013). Deciphering tectonic phases of the Amundsen Sea embayment shelf, West Antarctica, from a magnetic anomaly grid. *Tectonophysics*, 585, 113–123. <https://doi.org/10.1016/j.tecto.2012.06.036>
- Grindley, G. W., & Davey, F. J. (1982). The reconstruction of New Zealand, Australia, and Antarctica. In C. Craddock (Ed.), *Antarctic geoscience* (pp. 15–29). Madison, WI: University of Wisconsin Press.
- Grobys, J., Gohl, K., Davy, B., Uenzelmann-Neben, G., Deen, T., & Barker, D. (2007). Is the Bounty Trough off eastern New Zealand an aborted rift? *Journal of Geophysical Research*, 112, B03103. <https://doi.org/10.1029/2005JB004229>
- Grobys, J. W., Gohl, K., & Eagles, G. (2008). Quantitative tectonic reconstructions of Zealandia based on crustal thickness estimates. *Geochemistry, Geophysics, Geosystems*, 9, Q01005. <https://doi.org/10.1029/2007GC001691>
- Grobys, J. W., Gohl, K., Uenzelmann-Neben, G., Davy, B., & Barker, D. (2009). Extensional and magmatic nature of the Campbell Plateau and Great South basin from deep crustal studies. *Tectonophysics*, 472(1–4), 213–225. <https://doi.org/10.1016/j.tecto.2008.05.003>
- Heine, C., & Brune, S. (2014). Oblique rifting of the equatorial Atlantic: Why there is no Saharan Atlantic Ocean. *Geology*, 42(3), 211–214.
- Herzer, R. H., & Wood, R. A. (1988). The geology and structure of Mernoo Bank and surrounding area, western Chatham Rise. *New Zealand Geological Survey Record*, 29, 22.
- Horstwood, M. S. A., Košler, J., Gehrels, G., Jackson, S. E., McLean, N. M., Paton, C., et al. (2016). Community-derived standards for LA-ICP-MS U-(Th-) Pb geochronology—Uncertainty propagation, age interpretation and data reporting. *Geostandards and Geoanalytical Research*, 40(3), 311–332. <https://doi.org/10.1111/j.1751-908X.2016.00379.x>
- Hunt, T. M. (1978). Stokes Magnetic Anomaly System. *New Zealand Journal of Geology and Geophysics*, 21(5), 595–606. <https://doi.org/10.1080/00288306.1978.10424087>
- Ireland, T. R., & Williams, I. S. (2003). Considerations in zircon geochronology by SIMS. *Reviews in Mineralogy and Geochemistry*, 53(1), 215–241. <https://doi.org/10.2113/0530215>
- Jaffey, A. H., Flynn, K. F., Glendenin, L. E., Bentley, W. C., & Essling, A. M. (1971). Precision measurement of half-lives and specific activities of  $^{235}\text{U}$  and  $^{238}\text{U}$ . *Physical Review C*, 4(5), 1889–1906.
- Jochum, K. P., Weis, U., Stoll, B., Kuzmin, D., Yang, Q., Raczek, I., et al. (2011). Determination of reference values for NIST SRM 610–617 glasses following ISO guidelines. *Geostandards and Geoanalytical Research*, 35(4), 397–429. <https://doi.org/10.1111/j.1751-908X.2011.00120.x>
- Keeman, J., & Palin, J. M. (2013). Determining the provenance of the Murihiku terrane using igneous clasts from Jurassic and Triassic conglomerates, Catlins coast, New Zealand. *Geoscience Society of New Zealand Miscellaneous Publication*, 136A, 54.
- Kimbrough, D. L., Tulloch, A. J., Coombs, D. S., Landis, C. A., Johnston, M. R., & Mattinson, J. M. (1994). Uranium-lead zircon ages from the Median Tectonic Zone, New Zealand. *New Zealand Journal of Geology and Geophysics*, 37, 393–419.
- Kipf, A., Mortimer, N., Werner, R., Gohl, K., van den Boogaard, P., Hauff, F., & Hoernle, K. (2012). Granitoids and dykes of the Pine Island Bay region, West Antarctica. *Antarctic Science*, 24(05), 473–484. <https://doi.org/10.1017/S0954102012000259>
- Klepeis, K. A., King, D., De Paoli, M., Clarke, G. L., & Gehrels, G. (2007). Interaction of strong lower and weak middle crust during lithospheric extension in western New Zealand. *Tectonics*, 26, TC4017. <https://doi.org/10.1029/2006TC002003>
- Klepeis, K. A., Schwartz, J., Stowell, H., & Tulloch, A. J. (2016). Gneiss domes, vertical and horizontal mass transfer, and the initiation of extension in the hot lower-crustal root of a continental arc, Fiordland, New Zealand. *Lithosphere*, 8(2), 116–140. <https://doi.org/10.1130/L490.1>
- Krogh, T. E. (1982). Improved accuracy of U-Pb zircon dating by selection of more concordant fractions using a high-gradient magnetic separation technique. *Geochimica et Cosmochimica Acta*, 46(4), 631–635. [https://doi.org/10.1016/0016-7037\(82\)90164-8](https://doi.org/10.1016/0016-7037(82)90164-8)

- Kula, J., Tulloch, A. J., Spell, T. L., & Wells, M. L. (2007). Two-stage rifting of Zealandia-Australia-Antarctica: Evidence from  $^{40}\text{Ar}/^{39}\text{Ar}$  thermochronometry of the Sisters Shear Zone, Stewart Island, New Zealand. *Geology*, 35(5), 411–414. <https://doi.org/10.1130/G23432A.1>
- Kula, J., Tulloch, A. J., Spell, T. L., Wells, M. L., & Zanetti, K. (2009). Thermal evolution of the Sisters Shear Zone, southern New Zealand; formation of the Great South basin and onset of Pacific-Antarctic spreading. *Tectonics*, 28, TC5015. <https://doi.org/10.1029/2008TC002368>
- Lamb, S., Mortimer, N., Smith, E., & Turner, G. (2016). Focusing of relative plate motion at a continental transform fault: Cenozoic dextral displacement > 700 km on New Zealand's Alpine Fault, reversing > 225 km of Late Cretaceous sinistral motion. *Geochemistry, Geophysics, Geosystems*, 17, 1197–1213. <https://doi.org/10.1002/2015GC006225>
- Lisker, F., & Olesch, M. (1998). *Cooling and denudation history of western Marie Byrd Land, Antarctica, based on apatite fission-track advances in fission-track geochronology* (pp. 225–240). Dordrecht, Netherlands: Springer.
- Liu, J., Scott, J. M., Martin, C. E., & Pearson, D. G. (2015). The longevity of Archean mantle residues in the convecting upper mantle and their role in young continent formation. *Earth and Planetary Science Letters*, 424, 109–118. <https://doi.org/10.1016/j.epsl.2015.05.027>
- Ludwig, K. (2011). *Isoplot v. 4.15: a geochronological toolkit for Microsoft Excel*: Berkeley (p. 70). California: Berkeley Geochronology Center Special Publication 4.
- Luyendyk, B. P., Wilson, D. S., & Siddoway, C. S. (2003). Eastern margin of the Ross Sea rift in western Marie Byrd Land, Antarctica: Crustal structure and tectonic development. *Geochemistry, Geophysics, Geosystems*, 4(10), 1090. <https://doi.org/10.1029/2002GC000462>
- Maas, R., Grew, E. S., & Carson, C. J. (2015). Isotopic constraints (Pb, Rb-Sr, Sm-Nd) on the sources of Early Cambrian pegmatites with boron and beryllium minerals in the Larssen Hills, Prydz Bay, Antarctica. *The Canadian Mineralogist*, 53(2), 249–272. <https://doi.org/10.3749/canmin.1400081>
- MacKinnon, T. C. (1983). Origin of Torlesse terrane and coeval rocks, South Island, New Zealand. *Geological Society of America*, 94(8), 967–985. [https://doi.org/10.1130/0016-7606\(1983\)94<967:OOTTTA>2.0.CO;2](https://doi.org/10.1130/0016-7606(1983)94<967:OOTTTA>2.0.CO;2)
- Macpherson, C. G., Dreher, S. T., & Thirlwall, M. F. (2006). Adakites without slab melting: High pressure differentiation of island arc magma, Mindanao, the Philippines. *Earth and Planetary Science Letters*, 243(3–4), 581–593. <https://doi.org/10.1016/j.epsl.2005.12.034>
- McCoy-West, A. J., Bennett, V. C., & Amelin, Y. J. G. e. C. A. (2016). Rapid Cenozoic ingrowth of isotopic signatures simulating “HIMU” in ancient lithospheric mantle: Distinguishing source from process. *Geochimica et Cosmochimica Acta*, 187, 79–101.
- McCoy-West, A. J., Bennett, V. C., Puchtel, I. S., & Walker, R. J. (2013). Extreme persistence of cratonic lithosphere in the southwest Pacific: Paleoproterozoic Os isotopic signatures in Zealandia. *Geology*, 41(2), 231–234. <https://doi.org/10.1130/G33626.1>
- McFadden, R., Teyssier, C., Siddoway, C. S., Cosca, M., & Fanning, C. (2015). Mid-Cretaceous oblique rifting of West Antarctica: Emplacement and rapid cooling of the Fosdick Mountains migmatite-cored gneiss dome. *Lithos*, 232, 306–318. <https://doi.org/10.1016/j.lithos.2015.07.005>
- Mortimer, N. (2004). New Zealand's geological foundations. *Gondwana Research*, 7(1), 261–272. [https://doi.org/10.1016/S1342-937X\(05\)70324-5](https://doi.org/10.1016/S1342-937X(05)70324-5)
- Mortimer, N. (2014). The orocinal bend in the South Island, New Zealand. *Journal of Structural Geology*, 64, 32–38. <https://doi.org/10.1016/j.jsg.2013.08.011>
- Mortimer, N. (2018). Evidence for a pre-Eocene proto-Alpine Fault through Zealandia. *New Zealand Journal of Geology and Geophysics*, 61, 1–9.
- Mortimer, N., Campbell, H. J., Tulloch, A., King, P., Stagpoole, V., Wood, R., Rattenbury, M., et al. (2017). Zealandia: Earth's hidden continent. *GSA Today*, 27(3), 27–35. <https://doi.org/10.1130/GSATG321A.1>
- Mortimer, N., Davey, F. J., Melhuish, A., Yu, J., & Godfrey, N. J. (2002). Geological interpretation of a deep seismic reflection profile across the Eastern Province and Median Batholith, New Zealand: Crustal architecture of an extended Phanerozoic convergent orogen. *New Zealand Journal of Geology and Geophysics*, 45(3), 349–363. <https://doi.org/10.1080/00288306.2002.9514978>
- Mortimer, N., Gans, P. B., Meffre, S., Martin, C. E., Seton, M., Williams, S., et al. (2017). Regional volcanism of northern Zealandia: post-Gondwana break-up magmatism on an extended, submerged continent. In S. Sensarma & B. C. Storey (Eds.), *Large igneous provinces from Gondwana and adjacent regions*. Geological Society, London, Special Publication 463. London. <https://doi.org/10.1144/SP463.9>
- Mortimer, N., Hoernle, K., Hauff, F., Palin, J. M., Dunlap, W. J., Werner, R., & Faure, K. (2006). New constraints on the age and evolution of the Wishbone Ridge, southwest Pacific Cretaceous microplates, and Zealandia-West Antarctica breakup. *Geology*, 34(3), 185–188. <https://doi.org/10.1130/G22168.1>
- Mortimer, N., Kohn, B., Seward, D., Spell, T., & Tulloch, A. (2016). Reconnaissance thermochronology of southern Zealandia. *Journal of the Geological Society*, 173(2), 370–383. <https://doi.org/10.1144/jgs2015-021>
- Mortimer, N., Palin, J. M., Dunlap, W. J., & Hauff, F. (2011). Extent of the Ross orogen in Antarctica: New data from DSDP 270 and Iselin Bank. *Antarctic Science*, 23(03), 297–306. <https://doi.org/10.1017/S0954102010000969>
- Mortimer, N., Rattenbury, M. S., King, P. R., Bland, K. J., Barrell, D. J. A., Bache, F., et al. (2014). High-level stratigraphic scheme for New Zealand rocks. *New Zealand Journal of Geology and Geophysics*, 57(4), 402–419. <https://doi.org/10.1080/00288306.2014.946062>
- Mortimer, N., Tulloch, A. J., Spark, R. N., Walker, N. W., Ladley, E., & Kimbrough and Allibone, AH. (1999). Overview of the Median Batholith, New Zealand: A new interpretation of the geology of the Median Tectonic Zone and adjacent rocks. *Journal of African Earth Sciences*, 29(1), 257–268. [https://doi.org/10.1016/S0899-5362\(99\)00095-0](https://doi.org/10.1016/S0899-5362(99)00095-0)
- Mortimer, N., Turnbull, R., Palin, J., Tulloch, A., Rollet, N., & Hashimoto, T. (2015). Triassic–Jurassic granites on the Lord Howe rise, northern Zealandia. *Australian Journal of Earth Sciences*, 62, 735–742.
- Mortimer, N., van den Bogaard, P., Hoernle, K., Timm, C., Gans, P., Werner, R., & Rieftahl, F. (2019). Late Cretaceous oceanic plate reorganization and the breakup of Zealandia and Gondwana. *Gondwana Research*, 65, 31–42. <https://doi.org/10.1016/j.gr.2018.07.010>
- Muir, R., Weaver, S., Bradshaw, J., Eby, G., & Evans, J. (1995). The Cretaceous Separation Point batholith, New Zealand: Granitoid magmas formed by melting of mafic lithosphere. *Journal of the Geological Society*, 152(4), 689–701. <https://doi.org/10.1144/gsjgs.152.4.0689>
- Muir, R. J., Ireland, T. R., Weaver, S. D., & Bradshaw, J. D. (1994). Ion microprobe U-Pb zircon geochronology of granitic magmatism in the Western Province of the South Island, New Zealand. *Chemical Geology*, 113(1–2), 171–189. [https://doi.org/10.1016/0009-2541\(94\)90011-6](https://doi.org/10.1016/0009-2541(94)90011-6)
- Muir, R. J., Ireland, T. R., Weaver, S. D., & Bradshaw, J. D. (1996). Ion microprobe dating of Paleozoic granitoids: Devonian magmatism in New Zealand and correlations with Australia and Antarctica. *Chemical Geology: Isotope Geoscience*, 127, 191–210.
- Muir, R. J., Ireland, T. R., Weaver, S. D., Bradshaw, J. D., Evans, J. A., Eby, G. N., & Shelley, D. (1998). Geochronology and geochemistry of a Mesozoic magmatic arc system, Fiordland, New Zealand. *Journal of the Geological Society of London*, 155(6), 1037–1053. <https://doi.org/10.1144/gsjgs.155.6.1037>
- Mukasa, S. B., & Dalziel, I. W. D. (2000). Marie Byrd Land, West Antarctica: Evolution of Gondwana's Pacific margin constrained by zircon U-Pb geochronology and feldspar common-Pb isotopic compositions. *Geological Society of America Bulletin*, 112(4), 611–627. [https://doi.org/10.1130/0016-7606\(2000\)112<611:MBLWAE>2.0.CO;2](https://doi.org/10.1130/0016-7606(2000)112<611:MBLWAE>2.0.CO;2)

- Münker, C., & Cooper, R. (1999). The Cambrian arc complex of the Takaka terrane, New Zealand: An integrated stratigraphical, paleontological and geochemical approach. *New Zealand Journal of Geology and Geophysics*, 42(3), 415–445. <https://doi.org/10.1080/00288306.1999.9514854>
- Nakamura, N. (1974). Determination of REE, Ba, Fe, Mg, Na and K in carbonaceous and ordinary chondrites. *Geochimica et Cosmochimica Acta*, 38(5), 757–775. [https://doi.org/10.1016/0016-7037\(74\)90149-5](https://doi.org/10.1016/0016-7037(74)90149-5)
- Nelson, D., & Cottle, J. (2017). Long-term geochemical and geodynamic segmentation of the paleo-Pacific margin of Gondwana: Insight from the Antarctica and adjacent sectors. *Tectonics*, 36, 3229–3247. <https://doi.org/10.1002/2017TC004611>
- Pankhurst, R. J., Millar, I. L., Grunow, A. M., & Storey, B. C. (1993). The pre-Cenozoic magmatic history of the Thurston Island crustal block, West Antarctica. *Journal of Geophysical Research*, 98(B7), 11,835–11,849. <https://doi.org/10.1029/93JB01157>
- Pankhurst, R. J., Weaver, S. D., Bradshaw, J. D., Storey, B. C., & Ireland, T. R. (1998). Geochronology and geochemistry of pre-Jurassic superterranes in Marie Byrd Land, Antarctica. *Journal of Geophysical Research*, 103(B2), 2529–2547. <https://doi.org/10.1029/97JB02605>
- Panter, K. S., Blusztajn, J., Hart, S. R., Kyle, P. R., Esser, R., & McIntosh, W. C. (2006). The origin of HIMU in the SW Pacific: Evidence from intraplate volcanism in southern New Zealand and Subantarctic Islands. *Journal of Petrology*, 47(9), 1673–1704. <https://doi.org/10.1093/petrology/egl024>
- Paton, C., Hellstrom, J. C., Paul, B., Woodhead, J. D., & Hergt, J. M. (2011). Iolite: Freeware for the visualisation and processing of mass spectrometric data. *Journal of Analytical Atomic Spectrometry*, 26(12), 2508–2518.
- Paton, C., Woodhead, J. D., Hellstrom, J. C., Hergt, J. M., Greig, A., & Maas, R. (2010). Improved laser ablation U-Pb zircon geochronology through robust downhole fractionation correction. *Geochemistry, Geophysics, Geosystems*, 11, Q0AA06. <https://doi.org/10.1029/2009GC002618>
- Pearce, J. A., Harris, N. B., & Tindle, A. G. (1984). Trace element discrimination diagrams for the tectonic interpretation of granitic rocks. *Journal of Petrology*, 25(4), 956–983. <https://doi.org/10.1093/petrology/25.4.956>
- Phillips, C. J., Cooper, A. F., Palin, J. M., & Nathan, S. (2005). Geochronological constraints on Cretaceous–Paleocene volcanism in South Westland, New Zealand. *New Zealand Journal of Geology and Geophysics*, 48(1), 1–14. <https://doi.org/10.1080/00288306.2005.9515094>
- Pickett, D. A., & Wasserburg, G. (1989). Neodymium and strontium isotopic characteristics of New Zealand granitoids and related rocks. *Contributions to Mineralogy and Petrology*, 103(2), 131–142. <https://doi.org/10.1007/BF00378499>
- Price, R., Spandler, C., Arculus, R., & Reay, A. (2011). The Longwood igneous complex, Southland, New Zealand: A Permo-Jurassic, intra-oceanic, subduction-related, I-type batholithic complex. *Lithos*, 126(1–2), 1–21. <https://doi.org/10.1016/j.lithos.2011.04.006>
- Price, R. C., Ireland, T. R., Maas, R., & Arculus, R. J. (2006). SHRIMP ion probe zircon geochronology and Sr and Nd isotope geochemistry for southern Longwood Range and Bluff Peninsula intrusive rocks of Southland, New Zealand. *New Zealand Journal of Geology and Geophysics*, 49(3), 291–303. <https://doi.org/10.1080/00288306.2006.9515168>
- Raine, J. I., Kennedy, E. M., Griffin, A. G., & Clowes, C. D. (2018). Materials for improved assessment of the petroleum source potential of New Zealand coaly rocks. 1. Mid-Cretaceous stratigraphy, coal abundance, flora and climate. *GNS science report 2018/07*, 99p.
- Reyners, M., Eberhart-Phillips, D., Upton, P., & Gubbins, D. (2017). Three-dimensional imaging of impact of a large igneous province with a subduction zone. *Earth and Planetary Science Letters*, 460, 143–151. <https://doi.org/10.1016/j.epsl.2016.12.025>
- Richard, S. M., Smith, C. H., Kimbrough, D. L., Fitzgerald, P. G., Luyendyk, B. P., & McWilliams, M. O. (1994). Cooling history of the northern Ford Ranges, Marie Byrd Land, West Antarctica. *Tectonics*, 13(4), 837–857. <https://doi.org/10.1029/93TC03322>
- Ring, U., Bernet, M., & Tulloch, A. (2015). Kinematic, finite strain and vorticity analysis of the Sisters Shear Zone, Stewart Island, New Zealand. *Journal of Structural Geology*, 73, 114–129. <https://doi.org/10.1016/j.jsg.2015.02.004>
- Roser, B. P., Cooper, R. A., Nathan, S., & Tulloch, A. J. (1996). Reconnaissance sandstone geochemistry, provenance, and tectonic setting of the lower Paleozoic terranes of the West coast and Nelson, New Zealand. *New Zealand Journal of Geology and Geophysics*, 39(1), 1–16. <https://doi.org/10.1080/00288306.1996.9514690>
- Sagar, M., & Palin, J. M. (2011). Emplacement, metamorphism, deformation and affiliation of mid-Cretaceous orthogneiss from the Paparoa Metamorphic Core Complex lower-plate, Charleston, New Zealand. *New Zealand Journal of Geology and Geophysics*, 54(3), 273–289. <https://doi.org/10.1080/00288306.2011.562904>
- Sahoo, T., King, P., Bland, K., Strogen, D., Sykes, R., & Bache, F. (2014). Tectono-sedimentary evolution and source rock distribution of the mid to Late Cretaceous succession in the Great South basin, New Zealand. *The APPEA Journal*, 54(1), 259–274. <https://doi.org/10.1071/AJ13026>
- Sandwell, D. T., & Smith, W. H. F. (1997). Marine gravity anomaly from Geosat and ERS I satellite altimetry. *Journal of Geophysical Research*, 102(B5), 10,039–10,054. <https://doi.org/10.1029/96JB03223>
- Schmitz, M. D., Bowring, S. A., & Ireland, T. R. (2003). Evaluation of Duluth Complex anorthositic series (AS3) zircon as a U-Pb geochronological standard: New high-precision isotope dilution thermal ionization mass spectrometry results. *Geochimica et Cosmochimica Acta*, 67(19), 3665–3672. [https://doi.org/10.1016/S0016-7037\(03\)00200-X](https://doi.org/10.1016/S0016-7037(03)00200-X)
- Schoene, B., Crowley, J. L., Condon, D. J., Schmitz, M. D., & Bowring, S. A. (2006). Reassessing the uranium decay constants for geochronology using ID-TIMS U-Pb data. *Geochimica et Cosmochimica Acta*, 70(2), 426–445. <https://doi.org/10.1016/j.gca.2005.09.007>
- Schulte, D. O., Ring, U., Thomson, S. N., Glodny, J., & Carrad, H. (2014). Two-stage development of the Paparoa Metamorphic Core Complex, West coast, South Island, New Zealand: Hot continental extension precedes sea-floor spreading by ~25 my. *Lithosphere*, 6(3), 177–194. <https://doi.org/10.1130/L348.1>
- Schwartz, J. J., Klepeis, K. A., Sadorski, J. F., Stowell, H. H., Tulloch, A. J., & Coble, M. A. (2017). The tempo of continental arc construction in the Mesozoic Median Batholith, Fiordland, New Zealand. *Lithosphere*, 9(3), 343–365. <https://doi.org/10.1130/L610.1>
- Scott, J., & Cooper, A. J. T. (2006). Early Cretaceous extensional exhumation of the lower crust of a magmatic arc: Evidence from the Mount Irene shear zone, Fiordland, New Zealand. *Tectonics*, 25, TC2018. <https://doi.org/10.1029/2005TC001890>
- Scott, J., Waught, T. E., van der Meer, Q. H. A., Palin, J. M., Cooper, A. F., & Müunker, C. (2014). Metasomatized ancient lithospheric mantle beneath the young Zealandia microcontinent and its role in HIMU-like intraplate magmatism. *Geochemistry, Geophysics, Geosystems*, 15, 3477–3501. <https://doi.org/10.1002/2014GC005300>
- Scott, J. M. (2013). A review of the location and significance of the boundary between the Western Province and Eastern Province, New Zealand. *New Zealand Journal of Geology and Geophysics*, 56(4), 276–293. <https://doi.org/10.1080/00288306.2013.812971>
- Scott, J. M., Hodgkinson, A., Palin, J., Waught, T. E., Van der Meer, Q., & Cooper, A. F. (2014). Ancient melt depletion overprinted by young carbonatitic metasomatism in the New Zealand lithospheric mantle. *Contributions to Mineralogy and Petrology*, 167(1), 963. <https://doi.org/10.1007/s00410-014-0963-0>

- Scott, J. M., Turnbull, I., Auer, A., & Palin, J. M. (2013). The sub-Antarctic antipodes volcano: A <0.5 Ma HIMU-like Surtseyan volcanic outpost on the edge of the Campbell Plateau, New Zealand. *New Zealand Journal of Geology and Geophysics*, 56(3), 134–153. <https://doi.org/10.1080/00288306.2013.802246>
- Scott, J. M., Turnbull, I. M., Sagar, M. W., Tulloch, A. J., Waught, T. E., & Palin, J. M. (2015). Geology and geochronology of the sub-Antarctic Snares Islands/Tini Heke, New Zealand. *New Zealand Journal of Geology and Geophysics*, 58(2), 202–212. <https://doi.org/10.1080/00288306.2015.1023810>
- Siddoway, C. (2008). Tectonics of the West Antarctic Rift system: New light on the history and dynamics of distributed intracontinental extension. In A. K. Cooper (Ed.), *Antarctica: A keystone in a changing world* (pp. 91–114). Washington, DC: National Academies Press.
- Siddoway, C. S., Baldwin, S. L., Fitzgerald, P. G., Fanning, C. M., & Luyendyk, B. P. (2004). Ross Sea mylonites and the timing of intra-continental extension within the West Antarctic rift system. *Geology*, 32, 57–60.
- Siddoway, C. S., & Fanning, C. M. (2009). Paleozoic tectonism on the East Gondwana margin: Evidence from SHRIMP U-Pb zircon geochronology of a migmatite-granite complex in West Antarctica. *Tectonophysics*, 477, 262–277.
- Spell, T., McDougall, I., & Tulloch, A. J. (2000). Thermochronologic constraints on the breakup of the Pacific Gondwana margin: The Paparoa Metamorphic Core Complex, South Island, New Zealand. *Tectonics*, 19, 433–451.
- Steiger, R. H., & Jäger, E. (1977). Subcommission on geochronology: Convention on the use of decay constants in geo- and cosmochronology. *Earth and Planetary Science Letters*, 36(3), 359–362. [https://doi.org/10.1016/0012-821X\(77\)90060-7](https://doi.org/10.1016/0012-821X(77)90060-7)
- Storey, B. C., Leat, P. T., Weaver, S. D., Pankhurst, R. J., Bradshaw, J. D., & Kelley, S. (1999). Mantle plumes and Antarctica-New Zealand rifting: Evidence from mid-Cretaceous mafic dykes. *Journal of the Geological Society*, 156(4), 659–671. <https://doi.org/10.1144/gsjgs.156.4.0659>
- Strogen, D. P., Seebeck, H., Nicol, A., & King, P. R. (2017). Two-phase Cretaceous–Paleocene rifting in the Taranaki Basin region, New Zealand; implications for Gondwana break-up. *Journal of the Geological Society*, 174(5), 929–946. <https://doi.org/10.1144/jgs2016-160>
- Summerhayes, C. P. (1969). *Marine geology of the New Zealand subantarctic sea floor*, DSIR Bulletin 190. Wellington: Department of Scientific and Industrial Research.
- Sutherland, R. (1999). Basement geology and tectonic development of the greater New Zealand region: An interpretation from regional magnetic data. *Tectonophysics*, 308(3), 341–362. [https://doi.org/10.1016/S0040-1951\(99\)00108-0](https://doi.org/10.1016/S0040-1951(99)00108-0)
- Timm, C., Hoernle, K., Werner, R., Hauff, F., van den Bogaard, P., White, J., Mortimer, N., et al. (2010). Temporal and geochemical evolution of the Cenozoic intraplate volcanism of Zealandia. *Earth-Science Reviews*, 98(1–2), 38–64. <https://doi.org/10.1016/j.earscirev.2009.10.002>
- Tulloch, A. J. (1988). Batholiths, plutons, and suites: Nomenclature for granitoid rocks of Westland-Nelson, New Zealand. *New Zealand Journal of Geology and Geophysics*, 31(4), 505–509. <https://doi.org/10.1080/00288306.1988.10422147>
- Tulloch, A. J. (1991). Alkaline plutonic and volcanic rocks of the Late Cretaceous Mandamus Igneous Complex, North Canterbury. *Research Notes* 43, 15–23. NZ Geological Survey, Lower Hutt.
- Tulloch, A. J., Beggs, M., Kula, J., Spell, T., & Mortimer, N. (2006). Cordillera Zealandia, the Sisters Shear Zone and their influence on the early development of the Great South basin. In *2006 New Zealand Petroleum Conference proceedings* (pp. 1–11). Wellington: Ministry of Economic Development.
- Tulloch, A. J., & Kimbrough, D. L. (1989). The Paparoa Metamorphic Core Complex, Westland-Nelson, New Zealand: Cretaceous extension associated with fragmentation of the Pacific margin of Gondwana. *Tectonics*, 8, 1217–1234.
- Tulloch, A. J., & Kimbrough, D. L. (2003). Paired plutonic belts in convergent margins and the development of high Sr/Y magmatism: The Peninsular Ranges Batholith of California and the Median Batholith of New Zealand. *Geological Society of America Special Papers*, 374, 275–295.
- Tulloch, A. J., Kimbrough, D. L., Landis, C. A., Mortimer, N., & Johnston, M. R. (1999). Brook Street Terrane-Median Tectonic Zone relationships: Evidence from Jurassic conglomerates. *New Zealand Journal of Geology and Geophysics*, 42(2), 279–293. <https://doi.org/10.1080/00288306.1999.9514845>
- Tulloch, A. J., & Palmer, K. (1990). Tectonic implications of granite cobbles from the mid Cretaceous Pororari group, SE Nelson, New Zealand. *New Zealand Journal of Geology and Geophysics*, 33, 5–18.
- Tulloch, A. J., & Rabone, S. D. C. (1993). Mo-bearing granodiorite porphyry plutons of the early Cretaceous Separation Point Suite West Nelson, New Zealand. *New Zealand Journal of Geology and Geophysics*, 36(4), 401–408. <https://doi.org/10.1080/00288306.1993.9514586>
- Tulloch, A. J., Ramezani, J., Kimbrough, D. L., Faure, K., & Allibone, A. H. (2009). U-Pb geochronology of mid-Paleozoic plutonism in western New Zealand: Implications for S-type granite generation and growth of the East Gondwana margin. *Geological Society of America Bulletin*, 121(9–10), 1236–1261. <https://doi.org/10.1130/B26272.1>
- Tulloch, A. J., Ramezani, J., Maas, R., & Turnbull, R. E. (2017). High precision CA-TIMS U-Pb zircon ages for Late Devonian granites and associated rhyolitic volcanic sequences in Victoria, Australia. In J. Veamcombe (Ed.), *granites2017@benella: extended abstracts: an Australian Institute of Geoscientists symposium organised in conjunction with Geoscientists Symposia, 25 to 28 September 2017* (Vol. 65, pp. 118–119). Benella, Victoria, Australia: Bulletin (Australian Institute of Geoscientists).
- Tulloch, A. J., Ramezani, J., Mortimer, N., Mortensen, J., van den Bogaard, P., & Maas, R. (2009). Cretaceous felsic volcanism in New Zealand and Lord Howe rise (Zealandia) as a precursor to final Gondwana breakup. In B. Wernicke & U. Ring (Eds.), *Extending a continent: Architecture, rheology and heat budget*, *Geological Society, London, Special Publication* 321 (pp. 89–118).
- Turnbull, I. M., Uruski, C. I., Anderson, H. J., Lindqvist, J. K., Scott, G. H., Morgans, H. E. G., et al. (1993). Cretaceous and Cenozoic sedimentary basins of Western Southland, South Island, New Zealand. *Institute of Geological and Nuclear Sciences Monograph*, 1, 56.
- Turnbull, R., Tulloch, A., Ramezani, J., & Jongens, R. (2016). Extension-facilitated pulsed SIA-type “flare-up” magmatism at 370 Ma along the Southeast Gondwana margin in New Zealand: Insights from U-Pb geochronology and geochemistry. *Geological Society of America Bulletin*, 128(9–10), 1500–1520.
- van der Meer, Q., Waught, T. E., Scott, J., & Münker, C. (2017). Variable sources for Cretaceous to recent HIMU and HIMU-like intraplate magmatism in New Zealand. *Earth and Planetary Science Letters*, 469, 27–41. <https://doi.org/10.1016/j.epsl.2017.03.037>
- van der Meer, Q. H. A., Storey, M., Scott, J. M., & Waught, T. E. (2016). Abrupt spatial and geochemical changes in lamprophyre magmatism related to Gondwana fragmentation prior, during and after opening of the Tasman Sea. *Gondwana Research*, 36, 142–156. <https://doi.org/10.1016/j.gr.2016.04.004>
- van der Meer, Q. H. A., Waught, T. E., Tulloch, A. J., Whitehouse, M. J., & Andersen, T. (2018). Magmatic evolution during the Cretaceous transition from subduction to continental break-up of the eastern Gondwana margin (New Zealand) documented by in-situ zircon O-Hf isotopes and bulk-rock Sr-Nd isotopes. *Journal of Petrology*, 59(5), 849–880. <https://doi.org/10.1093/petrology/egy047>

- Waught, T. E., Weaver, S. D., Ireland, T. R., Maas, R., Muir, R. J., & Shelley, D. (1997). Field characteristics, petrography, and geochronology of the Hohonu batholith and the adjacent Granite Hill complex, North Westland, New Zealand. *New Zealand Journal of Geology and Geophysics*, 40(1), 1–17. <https://doi.org/10.1080/00288306.1997.9514736>
- Waught, T. E., Weaver, S. D., Muir, R. J., Maas, R., & Eby, G. N. (1998). The Hohonu batholith of North Westland, New Zealand: Granitoid compositions controlled by source H<sub>2</sub>O contents and generated during tectonic transition. *Contributions to Mineralogy and Petrology*, 130(3-4), 225–239. <https://doi.org/10.1007/s004100050362>
- Wandres, A. M., Bradshaw, J. D., Weaver, S., Maas, R., Ireland, T., & Eby, N. (2004). Provenance analysis using conglomerate clast lithologies: A case study from the Pahau terrane of New Zealand. *Sedimentary Geology*, 167(1-2), 57–89. <https://doi.org/10.1016/j.sedgeo.2004.02.002>
- Wareham, C. D., Millar, I. L., & Vaughan, A. P. (1997). The generation of sodic granite magmas, western Palmer Land, Antarctic Peninsula. *Contributions to Mineralogy and Petrology*, 128(1), 81–96. <https://doi.org/10.1007/s004100050295>
- Wasserburg, G. J., Craig, H., Menard, H. W., Engel, A. E. J., & Engel, C. G. (1963). Age and composition of a Bounty Islands granite and age of a Seychelles Islands granite. *Journal of Geology*, 71(6), 785–789. <https://doi.org/10.1086/626954>
- Watson, E. B., & Jurewicz, S. R. (1984). Behaviour of alkalis during diffusive interaction of granitic xenoliths with basaltic magma. *Journal of Geology*, 92(2), 121–131. <https://doi.org/10.1086/628843>
- Watters, W. A., & Fleming, C. A. (1975). Petrography of rocks from the Western chain of the Snares Islands. *New Zealand Journal of Geology and Geophysics*, 18(3), 491–499. <https://doi.org/10.1080/00288306.1975.10421549>
- Weaver, S., Adams, C., Pankhurst, R., & Gibson, I. (1992). Granites of Edward VII Peninsula, Marie Byrd Land: Anorogenic magmatism related to Antarctic-New Zealand rifting. *Earth and Environmental Science Transactions of the Royal Society of Edinburgh*, 83(1-2), 281–290. <https://doi.org/10.1017/S0263593300007963>
- Whalen, J. B., Currie, K. L., & Chappell, B. W. (1987). A-type granites: Geochemical characteristics, discrimination and petrogenesis. *Contributions to Mineralogy and Petrology*, 95(4), 407–419. <https://doi.org/10.1007/BF00402202>
- Wobbe, F., Gohl, K., Chambord, A., & Sutherland, R. (2012). Structure and breakup history of the rifted margin of West Antarctica in relation to Cretaceous separation from Zealandia and Bellingshausen plate motion. *Geochemistry, Geophysics, Geosystems*, 13, Q04W12. <https://doi.org/10.1029/2011GC003742>
- Wombacher, F., & Münker, C. (2000). Pb, Nd, and Sr isotopes and REE systematics of Cambrian sediments from New Zealand: Implications for the reconstruction of the early Paleozoic Gondwana margin along Australia and Antarctica. *The Journal of Geology*, 108(6), 663–686. <https://doi.org/10.1086/317950>
- Wood, R., & Anderson, H. (1989). Basement structure at the Chatham Islands. *Journal of the Royal Society of New Zealand*, 19, 269–282.
- Yakymchuk, C., Brown, C. R., Brown, M., Siddoway, C. S., Fanning, C. M., & Korhonen, F. J. (2015). Paleozoic evolution of western Marie Byrd Land, Antarctica. *Geological Society of America Bulletin*, 127, 1464–1484.